ESAIM: M2AN 56 (2022) 2197–2238
https://doi.org/10.1051/m2an/2022079

ESAIM: Mathematical Modelling and Numerical Analysis
www.esaim-m2an.org

CANONICAL MEAN-FIELD MOLECULAR DYNAMICS DERIVED FROM QUANTUM MECHANICS

Xin Huang[1], Petr Plecháč[2,*], Mattias Sandberg[1] and Anders Szepessy[1]

Abstract. Canonical quantum correlation observables can be approximated by classical molecular dynamics. In the case of low temperature the *ab initio* molecular dynamics potential energy is based on the ground state electron eigenvalue problem and the accuracy has been proven to be $\mathcal{O}(M^{-1})$, provided the first electron eigenvalue gap is sufficiently large compared to the given temperature and M is the ratio of nuclei and electron masses. For higher temperature eigenvalues corresponding to excited electron states are required to obtain $\mathcal{O}(M^{-1})$ accuracy and the derivations assume that all electron eigenvalues are separated, which for instance excludes conical intersections. This work studies a mean-field molecular dynamics approximation where the mean-field Hamiltonian for the nuclei is the partial trace $h := \mathrm{Tr}\,(H\mathrm{e}^{-\beta H})/\mathrm{Tr}\,(\mathrm{e}^{-\beta H})$ with respect to the electron degrees of freedom and H is the Weyl symbol corresponding to a quantum many body Hamiltonian $\widehat{H}$. It is proved that the mean-field molecular dynamics approximates canonical quantum correlation observables with accuracy $\mathcal{O}(M^{-1} + t\epsilon^2)$, for correlation time t where ϵ^2 is related to the variance of mean value approximation h. Furthermore, the proof derives a precise asymptotic representation of the Weyl symbol of the Gibbs density operator using a path integral formulation. Numerical experiments on a model problem with one nuclei and two electron states show that the mean-field dynamics has similar or better accuracy than standard molecular dynamics based on the ground state electron eigenvalue.

Mathematics Subject Classification. 35Q40, 81Q20, 82C10.

Received December 3, 2021. Accepted September 20, 2022.

1. Classical approximation of canonical quantum observables

1.1. Introduction to the approximations

We study approximation of *quantum time-correlation observables* at the quantum canonical ensemble for a system consisting of nuclei (slow degrees of freedom) and electrons (fast degrees of freedom) at the inverse temperature $\beta = 1/(k_{\mathrm{B}}T)$, where k_{B} is the Boltzmann constant and $T > 0$ is the temperature. We work in Hartree atomic units in which the reduced Planck constant $\hbar = 1$, the electron charge $e = 1$, the Bohr radius $a_0 = 1$ and the electron mass $m_e = 1$. Thus the semiclassical parameter in the subsequent analysis is given by

Keywords and phrases. Quantum canonical ensemble, correlation observables, molecular dynamics, excited states, mean-field approximation, semi-classical analysis, Weyl calculus, path integral.

[1] Institutionen för Matematik, Kungl. Tekniska Högskolan, 10044 Stockholm, Sweden.

[2] Department of Mathematical Sciences, University of Delaware, Newark, DE 19716, USA.

*Corresponding author: plechac@udel.edu

the ratio of nucleus and electron masses M. For example, in the case of a proton–electron system the ratio is $M = m_p/m_e \approx 1836$.

The full quantum system is described by the Hamiltonian operator which includes the kinetic energy of nuclei and the electronic kinetic energy operator together with the operator describing interaction between electrons, with coordinates x_e, and nuclei, with coordinates x,

$$-\frac{1}{2M}\Delta_x - \frac{1}{2}\Delta_{x_e} + \widehat{V}_e(x, x_e).$$

In this work, in the spirit of Born-Oppenheimer (adiabatic) approximation, we replace the time evolution of electrons by the Schrödinger electron eigenvalue problem. We represent the electronic kinetic energy operator and the interaction operator, $\widehat{H}_e = -\frac{1}{2}\Delta_{x_e} + \widehat{V}_e(x, x_e)$ as a matrix-valued potential $\widehat{V}(x)$ obtained by a representation of the operator $-\frac{1}{2}\Delta_{x_e} + \widehat{V}_e(x, x_e)$ on a finite-dimensional (d-dimensional) subspace of suitable normalized electronic eigenfunctions $\{\phi_k\}_{k=1}^d$, as $V(x)_{k\ell} = \langle \phi_k, \widehat{H}_e(x, \cdot)\phi_\ell \rangle$, described precisely in Section 2. Hence we work with the Hamiltonian operator

$$\widehat{H} = -\frac{1}{2M}\Delta \otimes \mathrm{I} + V(x). \tag{1.1}$$

The first term $-\frac{1}{2M}\Delta_x \otimes \mathrm{I}$ represents the kinetic energy of the nuclei where I is the $d \times d$ identity matrix. The second term, $V(x)$, is the matrix-valued potential approximation to $\widehat{H}_e$ and does not depend on M. We assume that this finite-dimensional approximation of the electronic operator results in a Hermitian matrix-valued smooth confining potential $V : \mathbb{R}^N \to \mathbb{R}^{d\times d}$ that depends on the positions $x_i \in \mathbb{R}^3$ of nuclei $i = 1, 2, \ldots, N'$, where we set $N = 3N'$. For the sake of simplicity, we assume that the nuclei have the same mass; in the case with different nuclei masses M becomes a diagonal matrix, which can be transformed to the formulation (1.1) with the same mass by the change of coordinates $M_1^{1/2}\bar{x} = M^{1/2}x$.

The large nuclei/electron mass ratio $M \gg 1$ is the basis of semiclassical analysis and implies a separation of time scales, for which nuclei represent slow and electrons much faster degrees of freedom. The Weyl quantization takes this scale separation into account. In particular for the Hamiltonian operator $\widehat{H}$ the corresponding matrix valued Weyl symbol becomes $H(x, p) = \frac{1}{2}|p|^2\mathrm{I} + V(x)$ for the nuclei phase-space points $(x, p) \in \mathbb{R}^N \times \mathbb{R}^N$, as described more precisely in Section 2.

In order to study correspondence between the quantum time-correlation function and its classical counter part we work in Heisenberg representation for the time-dependent quantum observables given by self-adjoint operators $\widehat{A}_t$ and $\widehat{B}_t$. We employ the Weyl quantization to link the quantum dynamics given by the Heisenberg equation to classical Hamiltonian equations of motions on the phase space $(x, p) \in \mathbb{R}^N \times \mathbb{R}^N$ of nuclei positions and momenta and to averaging with respect to a suitable canonical Gibbs distribution on the phase space.

More precisely, given a quantum system defined by the Hamiltonian $\widehat{H}$ acting on wave functions in $L^2(\mathbb{R}^N, \mathbb{C}^d) \equiv [L^2(\mathbb{R}^N)]^d$ we denote $\widehat{\rho} = \mathrm{e}^{-\beta\widehat{H}}$ the density operator for a quantum Hamiltonian operator $\widehat{H}$ at the inverse temperature $\beta > 0$ and consider quantum correlation observables based on the normalized trace

$$\frac{\mathrm{Tr}\left(\widehat{A}_t\widehat{B}_0\mathrm{e}^{-\beta\widehat{H}}\right)}{\mathrm{Tr}\left(\mathrm{e}^{-\beta\widehat{H}}\right)}, \tag{1.2}$$

and the symmetrized version

$$\mathfrak{T}_{\mathrm{qm}}(t) := \frac{\mathrm{Tr}\left(\frac{1}{2}\left(\widehat{A}_t\widehat{B}_0 + \widehat{B}_0\widehat{A}_t\right)\mathrm{e}^{-\beta\widehat{H}}\right)}{\mathrm{Tr}\left(\mathrm{e}^{-\beta\widehat{H}}\right)}, \tag{1.3}$$

for quantum observables $\widehat{A}_t = \mathrm{e}^{\mathrm{i}tM^{1/2}\widehat{H}}\widehat{A}_0\mathrm{e}^{-\mathrm{i}tM^{1/2}\widehat{H}}$ and $\widehat{B}_0$ at times t and 0, respectively. That is, the quantum observables solve the Heisenberg-von Neumann equation $\mathrm{d}\widehat{A}_t/\,\mathrm{d}t = \mathrm{i}M^{1/2}[\widehat{H}, \widehat{A}_t]$, where $[\widehat{H}, \widehat{A}_t] = \widehat{H}\widehat{A}_t - \widehat{A}_t\widehat{H}$ is the commutator. Here $M^{-1/2}$ plays the role of the Planck constant $\hbar$. With this time scale the nuclei move a

distance of order one in unit time in the classical setting. The aim is to derive a mean-field molecular dynamics approximation

$$\mathfrak{T}_{\mathrm{md}}(t) := \frac{\int_{\mathbb{R}^{2N}} A_0(z_t(z_0))B_0(z_0)\mathrm{Tr}\left(\mathrm{e}^{-\beta H(z_0)}\right)\mathrm{d}z_0}{\int_{\mathbb{R}^{2N}} \mathrm{Tr}\left(\mathrm{e}^{-\beta H(z_0)}\right)\mathrm{d}z_0} \tag{1.4}$$

of the correlation function (1.3), where A_0 and B_0 are the Weyl symbols for the initial quantum observables and $z_t := (x_t, p_t)$ solves the Hamiltonian system

$$\begin{aligned} \dot{x}_t &= \nabla_p h(x_t, p_t), \\ \dot{p}_t &= -\nabla_x h(x_t, p_t), \end{aligned} \tag{1.5}$$

with the initial data $z_0 := (x_0, p_0) \in \mathbb{R}^{2N}$ of nuclei positions and momenta. The trace $\mathrm{Tr}\left(\mathrm{e}^{-\beta H(z_0)}\right)$ is over the space $\mathbb{R}^{d\times d}$ of $d \times d$ matrices which can be also viewed as the trace operator with respect to electron degrees of freedom under the finite dimensional approximation of the electronic Hamiltonian. On the other hand $\mathrm{Tr}\left(\mathrm{e}^{-\beta\widehat{H}}\right)$ represents the trace acting on the space of trace operators on $L^2(\mathbb{R}^N, \mathbb{C}^d)$ which we can view as the trace with respect to both nuclei and electron degrees of freedom.

Two main questions arise: (a) how should the mean field Hamiltonian approximation $h : \mathbb{R}^{2N} \to \mathbb{R}$ be chosen, and (b) how small is the corresponding estimate for the approximation error $\mathfrak{T}_{\mathrm{qm}} - \mathfrak{T}_{\mathrm{md}}$?

Assume $\Psi : \mathbb{R}^N \to \mathbb{C}^{d\times d}$ is a differentiable orthogonal matrix. Based on certain regularity assumptions on A_0, B_0, V and Ψ, we prove in Theorem 2.1 that for the mean-field Hamiltonian $h : \mathbb{R}^N \times \mathbb{R}^N \to \mathbb{R}$ defined by

$$h(z) := \frac{\mathrm{Tr}\left(H(z)\mathrm{e}^{-\beta H(z)}\right)}{\mathrm{Tr}\left(\mathrm{e}^{-\beta H(z)}\right)}, \tag{1.6}$$

and the symbols A_0 and B_0, which are independent of the electron coordinates, we have

$$|\mathfrak{T}_{\mathrm{qm}}(t) - \mathfrak{T}_{\mathrm{md}}(t)| = \mathcal{O}\big(M^{-1} + t\epsilon_1^2 + t^2\epsilon_2^2\big), \tag{1.7}$$

where the parameters ϵ_j^2 are the variances

$$\begin{aligned} \epsilon_1^2 &= \frac{\left\|\mathrm{Tr}\left((H-h)^2\mathrm{e}^{-\beta H}\right)\right\|_{L^1(\mathbb{R}^{2N})}}{\left\|\mathrm{Tr}\left(\mathrm{e}^{-\beta H}\right)\right\|_{L^1(\mathbb{R}^{2N})}}, \\ \epsilon_2^2 &= \frac{\left\|\mathrm{Tr}\left(\nabla(H_\Psi - h)\cdot\nabla(H_\Psi - h)\mathrm{e}^{-\beta H_\Psi}\right)\right\|_{L^1(\mathbb{R}^{2N})}}{\left\|\mathrm{Tr}\left(\mathrm{e}^{-\beta H_\Psi}\right)\right\|_{L^1(\mathbb{R}^{2N})}}, \end{aligned} \tag{1.8}$$

with the definition $H_\Psi(x,p) := \frac{|p|^2}{2}\mathrm{I} + \Psi^*(x)V(x)\Psi(x)$ using the Hermitian transpose $\Psi^*(x)$.

We note that the mean-field Hamiltonian can be written

$$\begin{aligned} h(x,p) &= \frac{|p|^2}{2} + \frac{\mathrm{Tr}\left(V(x)\mathrm{e}^{-\beta V(x)}\right)}{\mathrm{Tr}\left(\mathrm{e}^{-\beta V(x)}\right)} \\ &= \frac{|p|^2}{2} + \frac{\sum_{i=0}^{d-1}\lambda_i(x)\mathrm{e}^{-\beta\lambda_i(x)}}{\sum_{i=0}^{d-1}\mathrm{e}^{-\beta\lambda_i(x)}} =: \frac{|p|^2}{2} + \lambda_*(x), \end{aligned} \tag{1.9}$$

where $\lambda_i(x)$, $i = 0, \ldots, d-1$, are the eigenvalues of $V(x)$, and $\lambda_* : \mathbb{R}^N \to \mathbb{R}$ is the obtained mean-field potential. Therefore the mean-field h is independent of the large mass ratio parameter M, so that the dynamics (1.5) is independent of M and consequently the nuclei move a distance of order one in unit time. We see that the mean-field $h = \mathrm{Tr}\left(He^{-\beta H}\right)/\mathrm{Tr}\left(\mathrm{e}^{-\beta H}\right)$ is the mean value with respect to the Gibbs density. The error term ϵ_1^2 can be written as the corresponding normed variance

$$\epsilon_1^2 = \frac{\left\|\sum_{i=0}^{d-1}(\lambda_i - \lambda_*)^2\mathrm{e}^{-\beta\lambda_i}\right\|_{L^1(\mathbb{R}^N)}}{\left\|\sum_{i=0}^{d-1}\mathrm{e}^{-\beta\lambda_i}\right\|_{L^1(\mathbb{R}^N)}} \tag{1.10}$$

and at points x where the eigenvalues $\lambda_i(x)$ are separated a suitable choice of $\Psi(x)$ is the matrix of eigenvectors to $V(x)$ which implies

$$\mathrm{Tr}\left(\nabla(H_\Psi - h)\cdot\nabla(H_\Psi - h)\mathrm{e}^{-\beta H_\Psi}\right)(x,p) = \sum_{i=0}^{d-1}\left(\nabla(\lambda_i(x)-\lambda_*(x))\cdot\nabla(\lambda_i(x)-\lambda_*(x))\mathrm{e}^{-\beta\lambda_i(x)-\beta|p|^2/2}\right). \quad (1.11)$$

On the other hand to have sets with coinciding eigenvalues is generic in dimension two and higher, see [1], and there the matrix $\Psi(x)$ is in general not differentiable. Therefore (1.11) will typically not hold everywhere. Section 5 presents numerical experiments where also the size of the error terms are analyzed in different settings.

In Section 2 we review necessary background on Weyl calculus and state the main theoretical result, namely the error estimate (1.7), as Theorem 2.1, together with the ideas of its proof. Sections 3 and 4 present the proof of the theorem. Section 5 presents numerical experiments on the approximation error $\mathfrak{T}_{\mathrm{qm}}(t) - \mathfrak{T}_{\mathrm{md}}$ discussed in the next Section 1.2.

1.2. Numerical comparisons

In Section 5 we present some numerical examples with varying settings of $t, 1/M, \epsilon_i^2$, related to different potentials V with the purpose to study the following questions: Is the estimate (1.7) sharp or does the error in practise behave differently with respect to t, $1/M$ and ϵ_i^2? Is the main contribution to the error coming from approximation of the the matrix-valued potential by a scalar potential in the quantum setting or from the classical approximation of quantum dynamics based on scalar potentials? Can the mean-field dynamics improve approximation compared to using molecular dynamics based on the ground state eigenvalue λ_0 instead of λ_*?

Theorem 2.1 does not give precise answers to these questions. The aim of this section is to provide some insight from several numerical experiments on a model problem, chosen to avoid the computational difficulties for realistic systems with many particles. Therefore we use one nuclei in dimension one, $N = 1$, and two electron states, defined by the Hamiltonian

$$\widehat{H} = -\frac{1}{2M}\Delta\otimes\mathrm{I} + V(x), \quad (1.12)$$

where I is the 2×2 identity matrix, $V:\mathbb{R}\to\mathbb{R}^{2\times 2}$ given by

$$V(x) = \frac{1}{4}\left(x-\frac{1}{2}\right)^4\mathrm{I} + c\begin{bmatrix} x & \delta \\ \delta & -x\end{bmatrix}, \quad (x,c,\delta)\in\mathbb{R}\times\mathbb{R}\times\mathbb{R}, \quad (1.13)$$

with the two eigenvalues

$$\lambda_0(x) = \frac{1}{4}\left(x-\frac{1}{2}\right)^4 - c\sqrt{x^2+\delta^2}, \quad \lambda_1(x) = \frac{1}{4}\left(x-\frac{1}{2}\right)^4 + c\sqrt{x^2+\delta^2}, \quad (1.14)$$

plotted in Figure 1 (Case E in Tab. 1).

Section 5 presents numerical results comparing quantum mechanics to the three different numerical approximations based on: the ground state potential λ_0, mean-field potential λ_* and excited state dynamics. The excited state molecular dynamics studied in [2] uses several paths related to different electron eigenvalues and is defined by

$$\mathfrak{T}_{\mathrm{es}}(\tau) := \sum_{j=0}^{d-1}\int_{\mathbb{R}^{2N}} A_0(z_\tau^j(z_0))B_0(z_0)\frac{\mathrm{e}^{-\beta\left(\frac{|p_0|^2}{2}+\lambda_j(x_0)\right)}}{\sum_{k=0}^{d-1}\int_{\mathbb{R}^{2N}}\mathrm{e}^{-\beta\left(\frac{|p|^2}{2}+\lambda_k(x)\right)}\,\mathrm{d}x\,\mathrm{d}p}\,\mathrm{d}z_0, \quad (1.15)$$

where $z_\tau^j = (x_\tau^j, p_\tau^j)$, $j = 0,\ldots,d-1$ solves the Hamiltonian dynamics for state j

$$\begin{aligned}\dot{x}_\tau^j &= p_\tau^j,\\ \dot{p}_\tau^j &= -\nabla\lambda_j(x_\tau^j),\end{aligned}$$

with the initial condition $z_0^j = (x_0,p_0) = z_0$.

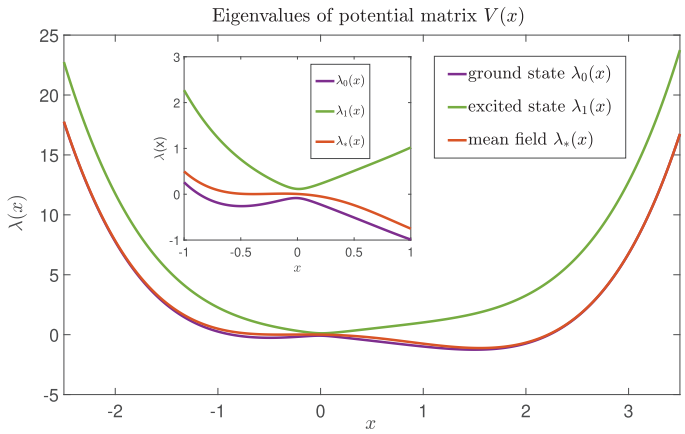

FIGURE 1. The eigenvalue functions $\lambda_0(x)$ and $\lambda_1(x)$ of the potential matrix $V(x)$, and the corresponding mean-field potential $\lambda_*(x)$, for the parameters $c = 1$, $\delta = 0.1$ (Case E).

1.2.1. Equilibrium observables

For equilibrium observables, *i.e.*, where $\tau = 0$, the mean-field and excited state dynamics are equal since then

$$\mathfrak{T}_{\mathrm{md}}(0) = \mathfrak{T}_{\mathrm{es}}(0) = \int_{\mathbb{R}^{2N}} A_0(z_0)B_0(z_0)\frac{\mathrm{Tr}\left(\mathrm{e}^{-\beta H(z_0)}\right)\mathrm{d}z_0}{\int_{\mathbb{R}^{2N}}\mathrm{Tr}\left(\mathrm{e}^{-\beta H(z)}\right)\mathrm{d}z}. \tag{1.16}$$

Numerical results on equilibrium observables show that mean-field and excited state molecular dynamics are more accurate than molecular dynamics based only on the ground state. In the case of correlation observables with $\tau > 0$, mean-field and excited state molecular dynamics give in general different approximations.

1.2.2. Correlation observables

Observations on quantum dynamics for a system in interaction with a heat bath at thermal equilibrium can be approximated by correlations (1.2) in the canonical ensemble, *cf.* [3–6]. For instance, the classical observable for the diffusion constant

$$\frac{1}{6\tau}\frac{3}{N}\sum_{k=1}^{N/3}|x_k(\tau) - x_k(0)|^2 = \frac{1}{2N\tau}\left(|x(\tau)|^2 + |x(0)|^2 - 2x(\tau)\cdot x(0)\right)$$

includes the time-correlation $x(\tau)\cdot x(0)$. Hence the corresponding quantum correlation (1.2) would for this case use $\widehat{A}_\tau = \widehat{x}_\tau \mathrm{I}$ and $\widehat{B}_0 = \widehat{x}_0\mathrm{I}$, and

$$\widehat{x}_\tau \cdot \widehat{x}_0 = \sum_{n=1}^{N/3}\sum_{j=1}^{3}\mathrm{e}^{\mathrm{i}\tau M^{1/2}\widehat{H}}\widehat{x}_{n_j}\mathrm{e}^{-\mathrm{i}\tau M^{1/2}\widehat{H}}\widehat{x}_{n_j}.$$

The numerical results in Section 5 for time-dependent observables are mainly based on the momentum auto-correlation

$$\frac{\mathrm{Tr}\left((\widehat{p}_\tau\cdot\widehat{p}_0 + \widehat{p}_0\cdot\widehat{p}_\tau)\mathrm{e}^{-\beta\widehat{H}}\right)}{2\mathrm{Tr}\left(\mathrm{e}^{-\beta\widehat{H}}\right)},$$

which is related to the diffusion constant D by the Green-Kubo formula [7]

$$D = \frac{\int_0^\infty\int_{\mathbb{R}^{2N}} p_s(x_0,p_0)\cdot p_0\mathrm{Tr}\left(\mathrm{e}^{-\beta H(x_0,p_0)}\right)\mathrm{d}x_0\,\mathrm{d}p_0\,\mathrm{d}s}{\int_{\mathbb{R}^{2N}}\mathrm{Tr}\left(\mathrm{e}^{-\beta H(x_0,p_0)}\right)\mathrm{d}x_0\,\mathrm{d}p_0},$$

TABLE 1. A summary of different parameter settings in each test case, where q_1 denotes the probability of the electronic excited state, with the precise definition in (5.4). Low value of β means a high system temperature, the parameter c measures the difference between the two eigenvalues $\gamma_\lambda := \int_{\mathbb{R}} |\lambda_1 - \lambda_0| \, \mathrm{e}^{-\beta\lambda_0} \, \mathrm{d}x / \int_{\mathbb{R}} \mathrm{e}^{-\beta\lambda_0} \, \mathrm{d}x$ and the parameters c and δ determine the eigenvalue gap. The value of ϵ_2^2 is computed following (1.11) with $\Psi(x)$ the matrix of eigenvectors to $V(x)$.

Case	β	c	δ	q_1	ϵ_1^2	ϵ_2^2	Plot	Features
A	3.3	1	1	0.0002	0.001	0.00013	Figure 6a	High β, large γ_λ, large gap
B	1	0.1	1	0.43	0.019	0.004	Figure 6b	Medium β, small γ_λ, small gap
C	1	0.1	0.01	0.46	0.009	0.010	Figure 6c	Medium β, small γ_λ, smallest gap
D	0.28	1	1	0.30	2.011	0.416	Figure 6d	Low β, large γ_λ, large gap
E	1	1	0.1	0.16	0.290	0.503	Figure 1	Medium β, large γ_λ, small gap

since the velocity is equal to the momentum in our case with unit particle mass.

The different numerical experiments in Table 1 are chosen by varying the parameters such that all three, two, one or no molecular dynamics approximate well. In Case A, with low temperature and large eigenvalue gap, all three molecular dynamics approximate the quantum observable with similar small error and also the error terms $1/M$, ϵ_1^2 and ϵ_2^2 are small. In Case B, with small difference of the eigenvalues (*i.e.*, c is small), the mean-field and excited states dynamics is more accurate than ground state dynamics and the error terms $1/M$, ϵ_1^2 and ϵ_2^2 are still small. The result is similar in Case C, with an avoided crossing (*i.e.*, δ is small) and small difference of the eigenvalues. In Case D, with high temperature and larger difference of the eigenvalues, only the excited state dynamics provides accurate approximations to the quantum observables and the error terms ϵ_1^2 and ϵ_2^2 are large. Finally in Case E, when the difference of the eigenvalues are sufficiently large and we have an avoided crossing, molecular dynamics is accurate only for short correlation time τ and the error terms ϵ_1^2 and ϵ_2^2 are large.

Figures 11b and 12b show that in Case D and Case E, where mean-field and ground state approximations are not accurate, the approximation error is dominated by the part corresponding to replacing the matrix valued potential by a scalar potential in the quantum formulation and not the part of the error resulting from classical approximation of quantum mechanics for scalar potentials. More precise conclusions relating the error terms $1/M$, $t\epsilon_1^2$ and $t^2\epsilon_2^2$ in (1.7) to the numerical experiments are in Section 5. The numerical experiments here also show that the mean-field dynamics has similar or better accuracy compared to ground state molecular dynamics. It would be interesting to do this comparison for realistic problems.

1.3. Relation to previous work

Classical approximation of canonical quantum correlation observables have been derived with $\mathcal{O}(M^{-1})$ accuracy for any temperature, see, *e.g.*, [2, 8]. Computationally this accuracy requires to solve classical molecular dynamics paths related to several electron eigenvalues, while the mean-field dynamics has the advantage to use only one classical path at the price of loosing accuracy over long time.

Classical limits of canonical quantum observables were first studied by Wigner [9]. His proof introduces the "Wigner" function for scalar Schrödinger equations and uses an expansion in the Planck constant $\hbar$ to relate equilibrium quantum observables to the corresponding classical Gibbs phase space averages.

To derive classical limits in the case of matrix or operator-valued Schrödinger equations previous works, see [8], diagonalize the electron eigenvalue problem, which then excludes settings where the eigenvalues coincide at certain points due to the inherent loss of regularity at such points. The mean-field formulation presented here avoids diagonalization of the electron eigenvalue problem at points with low eigenvalue regularity.

The classical limit with a scalar potential V, *e.g.*, the electron ground state eigenvalue, has been studied by three different methods:

(1) Solutions to the von Neumann quantum Liouville equation, for the density operator, are shown to converge to the solution of the classical Liouville equation, using the Wigner function [10], also under low regularity of the potential, *cf.* [11]. These results use the Wigner function and compactness arguments, which do not provide a convergence rate.
(2) In the second method, used in our work, the two main mathematical tools are a generalized version of Weyl's law and quantization properties, as described by semiclassical analysis, *e.g.*, in [12, 13]. The generalized Weyl's law links the trace for canonical quantum observables to classical phase space integrals, related to Wigner's work. The quantization properties compare the quantum and classical dynamics and provide convergence rates. Our study differs from previous works that also used similar tools, *e.g.*, [8, 14]. The standard method to bound remainder terms in semiclassical expansions, based on the Planck constant $\hbar$, use the Calderón-Vaillancourt theorem to estimate operator norms. Such approach yields error bounds with constants depending on the $L^1(\mathbb{R}^{2N})$-norms of Fourier transforms of symbols and the potential. The $L^1(\mathbb{R}^{2N})$-norm of a Fourier transformed function can be bounded by the $L^1(\mathbb{R}^{2N})$ norm of derivatives of order N of the function. Therefore the obtained constants in $\mathcal{O}(\hbar^\alpha)$ error estimates are large in high dimension N. In our work here we apply dominated convergence to obtain error estimates based on low regularity of symbols and the potential, while Fourier transforms in $L^1(\mathbb{R}^{2N})$ are only required to be finite and do not enter in the final error estimates.
(3) The third alternative in [15] provides a new method that also avoids the large constants in the Calderón-Vaillancourt theorem in high dimensions by using convergence with respect to a generalized Wasserstein distance and different weak topologies.

A computational bottleneck in *ab initio* molecular dynamics simulations of canonical correlation observables is in solving electron eigenvalue problems at each time step. An alternative to approximate quantum observables is to use path integral Monte Carlo formulations in order to evaluate Hamiltonian exponentials. The Hamiltonian exponentials come in two forms: oscillatory integrals in time $t \in \mathbb{R}$, based on $\mathrm{e}^{\mathrm{i}t\widehat{H}}$ for the dynamics, and integrals for Gibbs function $\mathrm{e}^{-\beta\widehat{H}}$ that decay with increasing inverse temperature $\beta \in (0, \infty)$. The high variance related to the oscillatory integrand $\mathrm{e}^{\mathrm{i}t\widehat{H}}$ means that standard computational path integral formulations for molecular dynamics are applied only to the statistics based on the partition function $\mathrm{Tr}\,(\mathrm{e}^{-\beta\widehat{H}})$ while the dynamics is approximated classically.

Two popular path integral methods are centroid molecular dynamics and ring-polymer molecular dynamics, see, *e.g.*, [16] or [17]. In these methods the discretized path integral is interpreted as a classical Hamiltonian with a particle/bead for each degree of freedom in the discretized path integral. For the centroid version the dynamics is based on the average of the particle/bead positions, *i.e.*, the centroid, with forces related to a free energy potential for the partition function thereby forming a mean-field approximation. It is related to the mean-field approximation (1.4) and (1.6) but differs in that in our work the forces are based on the mean Hamiltonian, for the partial trace over electron degrees of freedom, instead of on the partition function for the discretized path integral with respect to both nuclei and electron degrees of freedom, centered at the centroid. In ring-polymer molecular dynamics classical kinetic energy is added for each bead forming a Hamiltonian with harmonic oscillators in addition to the original potential energy. Consequently the phase-space is related to coupled ring polymers, one for each original particle.

There is so far no convergence proof for centroid nor ring-polymer molecular dynamics. Therefore it would be interesting to further study their relation to the mean-field model we analyse here. The mean-field formulation (1.4) and (1.6) can also offer an alternative to standard eigenvalue solutions by using a path integral formulation of the partial trace over the electron degrees of freedom, in the case of sufficiently large temperature avoiding the fermion sign problem, see, *e.g.*, [18]. Another difference to previous work is that the convergence proof here derives a precise asymptotic representation of the Weyl symbol for the Gibbs density operator using a path

integral formulation, providing an example that using path integrals for the Gibbs density can also result in simplification of the theory.

2. The main result and background from Weyl calculus

In this section we state the main theorem and review necessary tools from semiclassical analysis and functional integration.

To relate the quantum and classical observables we employ Weyl calculus for matrix-valued symbols. First, we introduce functional spaces that we use in the sequel:

(i) the Schwartz space of matrix-valued functions on the phase space

$$\mathcal{S} := \left\{ A \in C^\infty\big(\mathbb{R}^N \times \mathbb{R}^N, \mathbb{C}^{d\times d}\big) \mid \sup_{z\in\mathbb{R}^N\times\mathbb{R}^N} |z^\gamma \partial_z^\alpha A_{ij}(z)| < \infty, \text{ for all indices} \right\}$$

where we denote a point in the phase space $z = (x, p)$ and for a multi-index of non-negative integers $\alpha = (\alpha_1, \dots, \alpha_{2N})$, we have the partial derivatives $\partial_z^\alpha = \partial_{z_1}^{\alpha_1} \dots \partial_{z_{2N}}^{\alpha_{2N}}$ of the order $|\alpha| = \sum_i \alpha_i$ and similarly we have $z^\gamma = z_1^{\gamma_1} \dots z_{2N}^{\gamma_{2N}}$ for the multi-index γ. For a matrix-valued symbol A we also use the notation $A'(z)$ for the tensor $(A'(z))_{ij}^m := \partial_{z_m} A_{ij}(z)$ and $A''(z)$ for the 4th-order tensor $(A''(z))_{ij}^{mn} := \partial_{z_m z_n}^2 A_{ij}(z)$. The dual space of tempered distributions is denoted $\mathcal{S}'$.

(ii) the space of L^2 vector-valued wave functions

$$\mathcal{H} := L^2\big(\mathbb{R}^N, \mathbb{C}^d\big) \equiv \big[L^2\big(\mathbb{R}^N\big)\big]^d.$$

We define the Weyl quantization operator of a matrix-valued symbol $A \in \mathcal{S}$ as the mapping $A \mapsto \widehat{A}$ that assigns to the symbol A the linear operator $\widehat{A} : \mathcal{H} \to \mathcal{H}$ defined for all Schwartz functions $\phi(x)$ by

$$\begin{aligned} \widehat{A}\phi(x) &= \int_{\mathbb{R}^N} \left(\frac{\sqrt{M}}{2\pi}\right)^N \int_{\mathbb{R}^N} \mathrm{e}^{\mathrm{i}M^{1/2}(x-y)\cdot p} A\big(\tfrac{1}{2}(x+y), p\big)\, \mathrm{d}p\, \phi(y)\, \mathrm{d}y \\ &=: \int_{\mathbb{R}^N} K_A(x,y)\phi(y)\ \mathrm{d}y, \end{aligned} \tag{2.1}$$

and extended to all wave functions $\phi \in \mathcal{H}$ by density. The expression (2.1) shows that the kernel K_A on $\mathcal{H}$ is the Fourier transform in the second argument of the symbol $A(x, p)$ and consequently the Weyl quantization is well defined for symbols in $\mathcal{S}'$, the space of tempered distributions.

For example, the symbol

$$H(x,p) := \tfrac{1}{2}|p|^2 \mathrm{I} + V(x)$$

yields the Hamiltonian operator

$$\widehat{H} = -\frac{1}{2M}\Delta \otimes \mathrm{I} + V(x).$$

We formulate the main result as the following theorem estimating the mean-field approximation.

Theorem 2.1. *Let $\Psi : \mathbb{R}^N \to \mathbb{C}^{d\times d}$ be a differentiable mapping into orthogonal matrices and define $V_\Psi := \Psi^* V \Psi$, for the Hermitian potential $V : \mathbb{R}^N \to \mathbb{C}^{d\times d}$. Assume that the components of the Hessian V_Ψ'' are in the Schwartz class and the scalar symbols $a_0 : \mathbb{R}^{2N} \to \mathbb{C}$ and $b_0 : \mathbb{R}^{2N} \to \mathbb{C}$ are infinitely differentiable and compactly supported. Furthermore, suppose that there is a constant k such that $V + k\mathrm{I}$ is positive definite everywhere, $\operatorname{Tr}(\mathrm{e}^{-\beta\widehat{H}})$ is finite, and there is a constant C such that*

$$\big\|\operatorname{Tr} \mathrm{e}^{-\beta V}\big\|_{L^1(\mathbb{R}^N)} + \big\|\operatorname{Tr}\big(V^2 \mathrm{e}^{-\beta V}\big)\big\|_{L^1(\mathbb{R}^N)} + \left\| \operatorname{Tr}\left(\left(\sum_{m=1}^N \sum_{|\alpha|\le 3} \partial_{x_m}^\alpha V_\Psi \partial_{x_m}^\alpha V_\Psi \right) \mathrm{e}^{-\beta V_\Psi} \right) \right\|_{L^1(\mathbb{R}^N)} \le C,$$

$$\sum_{|\alpha|\le 3}\Big(\|\partial_z^\alpha a_0\|_{L^\infty(\mathbb{R}^{2N})}+\|\partial_z^\alpha b_0\|_{L^\infty(\mathbb{R}^{2N})}\Big)\le C,$$

$$\max_i \sum_{|\alpha|\le 3}\|\partial_x^\alpha \partial_{x_i} h\|_{L^\infty(\mathbb{R}^{2N})}\le C,$$

$$\int_{\mathbb{R}^{2N}} \operatorname{Tr}\left(\left|\sum_{n,m} p_n \partial^2_{x_n x_m} V_\Psi(x) p_m\right| \mathrm{e}^{-\beta\left(\frac{|p|^2}{2}\mathrm{I}+V_\Psi(x)\right)}\right)\mathrm{d}x\,\mathrm{d}p\le C,$$

$$\int_{\mathbb{R}^{2N}} \operatorname{Tr}\left(\left(\sum_n p_n \partial^2_{x_n} V_\Psi(x)\right)^2 \mathrm{e}^{-\beta\left(\frac{|p|^2}{2}\mathrm{I}+V_\Psi(x)\right)}\right)\mathrm{d}x\,\mathrm{d}p\le C,$$

then there are constants $c,\bar{M},\bar{t}$*, depending on* C *and* β*, such that the quantum canonical observable* (1.3)*, with* $A_0=a_0\mathrm{I}$ *and* $B_0=b_0\mathrm{I}$*, can be approximated by the mean-field molecular dynamics* (1.4), (1.5) *with the error*

$$|\mathfrak{T}_{\mathrm{qm}}(t)-\mathfrak{T}_{\mathrm{md}}(t)|\le c\big(M^{-1}+t\epsilon_1^2+t^2\epsilon_2^2\big), \tag{2.2}$$

for $M\ge\bar{M}$ *and* $0\le t\le\bar{t}$*, where*

$$\epsilon_1^2=\big\|\operatorname{Tr}\big((H-h)^2\mathrm{e}^{-\beta H}\big)\big\|_{L^1(\mathbb{R}^{2N})}/\big\|\operatorname{Tr}\big(\mathrm{e}^{-\beta H}\big)\big\|_{L^1(\mathbb{R}^{2N})},$$

$$\epsilon_2^2=\big\|\operatorname{Tr}\big(\nabla(H_\Psi-h)\cdot\nabla(H_\Psi-h)\mathrm{e}^{-\beta H_\Psi}\big)\big\|_{L^1(\mathbb{R}^{2N})}/\big\|\operatorname{Tr}\big(\mathrm{e}^{-\beta H}\big)\big\|_{L^1(\mathbb{R}^{2N})},\quad H_\Psi:=\frac{|p|^2}{2}\mathrm{I}+V_\Psi.$$

2.1. Overview and background to the proof

This section provides background and motivation to the proof of the theorem in three subsections. The first subsection reviews application of Weyl calculus for the dynamics, the second one is on a generalized form of Weyl's law in order to relate the quantum trace to phase space integrals and the third subsection introduces path integrals and their application in the context of our result.

2.1.1. Weyl calculus and dynamics

This section first introduces the central relation between commutators and corresponding Poisson brackets for the classical limit of dynamics. Given two smooth functions $v(x,p)$, $w(x,p)$ on the phase space we define the Poisson bracket

$$\begin{aligned}\{v,w\}&:=\nabla_p v(x,p)\cdot\nabla_x w(x,p)-\nabla_x v(x,p)\cdot\nabla_p w(x,p)\\&=(\nabla_{p'},-\nabla_{x'})\cdot(\nabla_x,\nabla_p)v(x',p')w(x,p)\big|_{(x,p)=(x',p')}.\end{aligned} \tag{2.3}$$

We denote the gradient operator in the variable $z=(x,p)$ as $\nabla_z=(\nabla_x,\nabla_p)$ and $\nabla'_z=(\nabla_p,-\nabla_x)$, hence the Poisson bracket is expressed as

$$\{v,w\}=(\nabla'_{z'}\cdot\nabla_z)v(z')w(z)\big|_{z=z'}. \tag{2.4}$$

For two operators $\widehat{C}$, $\widehat{D}$ on the space $\mathcal{H}$ we define their commutator

$$\left[\widehat{C},\widehat{D}\right]=\widehat{C}\widehat{D}-\widehat{D}\widehat{C}.$$

To relate the quantum and classical dynamics for particular observables with symbols of the type $a_0\mathrm{I}$ treated in Theorem 2.1, we assume that the classical Hamiltonian flow $z_t(z_0):=(x_t(z_0),p_t(z_0))$ solves the Hamiltonian system

$$\begin{aligned}\dot{x}_t&=p_t=\nabla_p h(x_t,p_t),\\ \dot{p}_t&=-\nabla_x h(x_t,p_t),\end{aligned}$$

with the initial data $(x_0, p_0) = z_0 \in \mathbb{R}^{2N}$. Given a scalar Schwartz function a_0 we define a smooth function on the flow $z_t(z_0)$

$$a_t(z_0) := a_0(z_t(z_0)), \tag{2.5}$$

and we have that $a_t(z_0)$ satisfies

$$\partial_t a_t(z_0) = \{h(z_0), a_t(z_0)\} \tag{2.6}$$

since the direct calculation gives

$$\partial_t a_t(z_0) = \partial_s a_0(z_t(z_s))\big|_{s=0} = \dot{z}_0 \cdot \nabla_{z_0} a_0(z_t(z_0)) = \{h(z_0), a_t(z_0)\}.$$

The corresponding quantum evolution of the observable $\widehat{A}$, for $t \in \mathbb{R}$, is defined by the Heisenberg-von Neumann equation

$$\partial_t \widehat{A}_t = \mathrm{i}M^{1/2}\Big[\widehat{H}, \widehat{A}_t\Big], \tag{2.7}$$

which implies the representation

$$\widehat{A}_t = \mathrm{e}^{\mathrm{i}tM^{1/2}\widehat{H}}\widehat{A}_0\mathrm{e}^{-\mathrm{i}tM^{1/2}\widehat{H}}.$$

The basic property in Weyl calculus that links the quantum evolution (2.7) to the classical (2.6) is the relation

$$\mathrm{i}M^{1/2}\Big[\widehat{H}, \widehat{a}_t\Big] = \widehat{\{H, a_t\}} + \widehat{r}^a_t \tag{2.8}$$

where the remainder symbol r^a_t is small. In Lemma 3.2 we show that

$$\lim_{M\to\infty} Mr^a_s = \frac{1}{12}\Big(\nabla_{z_0} \cdot \nabla'_{z'_0}\Big)^3 H(z_0)a_0(z_s(z'_0))\big|_{z_0=z'_0}. \tag{2.9}$$

The main obstacle to establish the classical limit for dynamics based on the matrix-valued operator Hamiltonian $\widehat{H}$ is that matrix symbols do not commute, *i.e.*, $[H, A_t] \neq 0$, which implies the additional larger remainder $\mathrm{i}M^{1/2}[H, A_t]$ in (2.8). Therefore the usual semiclassical analysis perform approximate diagonalization of $[\widehat{H}, \widehat{A}_t]$, see [2, 8]. Diagonalization of V introduces eigenvectors that are not smooth everywhere unless the eigenvalues are separated, due to the inherent loss of regularity for eigenvectors corresponding to coinciding eigenvalues, see [1]. To have a conical intersection point with coinciding eigenvalues is generic in dimension two, and in higher dimensions the intersection is typically a co-dimension two set, see [1]. The non smooth diagonalization has been so far a difficult obstacle to handle with the tools of Weyl calculus. The aim in our work is therefore to avoid diagonalization everywhere by analyzing a mean-field approximation differently.

In order to apply (2.8) we use Duhamel's principle, see [19]: the inhomogeneous linear equation in the variable $A_t - a_t \equiv A_t - a_t\mathrm{I}$, where A_t satisfies the evolution (2.7) and a_t is defined by (2.5),

$$\begin{aligned}\partial_t\Big(\widehat{A}_t - \widehat{a_t}\Big) &= \mathrm{i}M^{1/2}\Big[\widehat{H}, \widehat{A}_t\Big] - \widehat{\{h, a_t\}} \\ &= \mathrm{i}M^{1/2}\Big[\widehat{H}, \widehat{A}_t - \widehat{a}_t\Big] + \mathrm{i}M^{1/2}\Big[\widehat{H}, \widehat{a}_t\Big] - \widehat{\{h, a_t\}}\end{aligned}$$

can be solved by integrating solutions to the homogeneous problem with respect to the inhomogeneity

$$\widehat{A}_t - \widehat{a}_t = \int_0^t \mathrm{e}^{\mathrm{i}M^{1/2}(t-s)\widehat{H}}\Big(\mathrm{i}M^{1/2}\Big[\widehat{H}, \widehat{a}_s\Big] - \widehat{\{h, a_s\}}\Big)\mathrm{e}^{-\mathrm{i}M^{1/2}(t-s)\widehat{H}}\,\mathrm{d}s. \tag{2.10}$$

The quantum statistics has a similar remainder term to (2.9), namely the difference $\rho - \mathrm{e}^{-\beta H}$ of the Weyl symbol ρ for the quantum Gibbs density operator $\widehat{\rho} = \mathrm{e}^{-\beta\widehat{H}}$ and the classical Gibbs density $\mathrm{e}^{-\beta H}$. To characterize asymptotic behaviour as $M \to \infty$ of this difference we employ representation of the symbol ρ based on Feynman–Kac path integral formulation, as presented in Section 2.1.3.

2.1.2. Generalized Weyl law

To link the quantum trace to a classical phase space integral we will use a generalized form of Weyl's law, see [8, 12]. The semiclassical analysis is based on the fact that the $\mathcal{H}$-trace of a Weyl operator, with a $d \times d$ matrix-valued symbol, is equal to the phase-space average of its symbol trace. Indeed we have by the definition of the integral kernel in (2.1) for $A \in \mathcal{S}$

$$\operatorname{Tr} \widehat{A} = \int_{\mathbb{R}^N} \operatorname{Tr} K_A(x,x)\,\mathrm{d}x = \left(\frac{\sqrt{M}}{2\pi}\right)^N \int_{\mathbb{R}^N}\int_{\mathbb{R}^N} \operatorname{Tr} A(x,p)\,\mathrm{d}p\,\mathrm{d}x. \tag{2.11}$$

In fact also the composition of two Weyl operators is determined by the phase-space average as follows, see [8].

Lemma 2.2. *The composition of two Weyl operators $\widehat{A}$ and $\widehat{B}$, with $A \in \mathcal{S}$ and $B \in \mathcal{S}$ satisfies*

$$\operatorname{Tr}\left(\widehat{A}\widehat{B}\right) = \left(\frac{\sqrt{M}}{2\pi}\right)^N \int_{\mathbb{R}^{2N}} \operatorname{Tr}\left(A(x,p)B(x,p)\right)\mathrm{d}x\,\mathrm{d}p,$$

where $A(x,p)B(x,p)$ is the matrix product of the two $d \times d$ matrices $A(x,p)$ and $B(x,p)$.

Proof. The well-known proof is a straight forward evaluation of the integrals involved in the composition of two kernels and it is given here for completeness. The kernel of the composition is

$$K_{AB}(x,y) = \left(\frac{\sqrt{M}}{2\pi}\right)^{2N} \int_{\mathbb{R}^{3N}} A\big(\tfrac{1}{2}(x+x'),p\big)B\big(\tfrac{1}{2}(x'+y),p'\big) \times \mathrm{e}^{iM^{1/2}\left((x-x')\cdot p+(x'-y)\cdot p'\right)}\,\mathrm{d}p'\,\mathrm{d}p\,\mathrm{d}x'$$

so that the trace of the composition becomes

$$\begin{aligned}
\operatorname{Tr}\left(\widehat{A}\widehat{B}\right) &= \int_{\mathbb{R}^N} \operatorname{Tr} K_{AB}(x,x)\,\mathrm{d}x \\
&= \left(\frac{\sqrt{M}}{2\pi}\right)^{2N} \int_{\mathbb{R}^{4N}} \operatorname{Tr}\left(A\big(\tfrac{1}{2}(x+x'),p\big)B\big(\tfrac{1}{2}(x'+x),p'\big)\right) \times \mathrm{e}^{iM^{1/2}\left((x-x')\cdot p+(x'-x)\cdot p'\right)}\,\mathrm{d}p'\,\mathrm{d}p\,\mathrm{d}x'\,\mathrm{d}x \\
&= \left(\frac{\sqrt{M}}{2\pi}\right)^{2N} \int_{\mathbb{R}^{4N}} \operatorname{Tr}\left(A(y,p)B(y,p')\right)\mathrm{e}^{iM^{1/2}y'\cdot(p-p')}\,\mathrm{d}p'\,\mathrm{d}p\,\mathrm{d}y'\,\mathrm{d}y \\
&= \left(\frac{\sqrt{M}}{2\pi}\right)^{N} \int_{\mathbb{R}^{2N}} \operatorname{Tr}\left(A(y,p)B(y,p)\right)\mathrm{d}p\,\mathrm{d}y,
\end{aligned}$$

using the change of variables $(y,y') = ((x+x')/2, x-x')$, which verifies the claim. □

The composition of three operators does not have a corresponding phase-space representation. We will instead use the composition operator # (Moyal product), defined by $\widehat{A}\widehat{B} = \widehat{A\#B}$, to reduce the number of Weyl quantizations to two, *e.g.*, as $\widehat{A}\widehat{B}\widehat{C}\widehat{D} = \widehat{A\#B}\,\widehat{C\#D}$. More precisely, the Moyal product of two symbols has the representation

$$A\#B = \mathrm{e}^{\frac{\mathrm{i}}{2M^{1/2}}\left(\nabla_{x'}\cdot\nabla_p - \nabla_x\cdot\nabla_{p'}\right)} A(x,p)B(x',p')\big|_{(x,p)=(x',p')}. \tag{2.12}$$

For general background we refer the reader to [12] or [13].

The isometry between Weyl operators with the Hilbert–Schmidt inner product, $\operatorname{Tr}(\widehat{A}^*\widehat{B})$, and the corresponding $L^2(\mathbb{R}^N \times \mathbb{R}^N, \mathbb{C}^{d\times d})$ symbols obtained by Lemma 2.2 shows how to extend from symbols in $\mathcal{S}$ to $L^2(\mathbb{R}^N \times \mathbb{R}^N, \mathbb{C}^{d\times d})$ by density of $\mathcal{S}$ in $L^2(\mathbb{R}^N \times \mathbb{R}^N, \mathbb{C}^{d\times d})$, see [8]. We will use the Hilbert–Schmidt norms $\|\widehat{A}\|^2_{\mathcal{HS}} = \operatorname{Tr}(\widehat{A}^*\widehat{A}) = \operatorname{Tr}(\widehat{A}^2)$ and $\|\operatorname{Tr} A^2\|_{L^2(\mathbb{R}^{2N})}$ to estimate Weyl operators and Weyl symbols, respectively.

We show in Lemma 3.2 that having the Weyl symbols and V'' in the Schwartz class imply that dominated convergence can be applied in the phase space integrals obtained from the generalized form of Weyl's law.

2.1.3. Feynman–Kac path integrals

In order to analyse the symbol ρ for the Gibbs density operator $\widehat{\rho} = \mathrm{e}^{-\beta\widehat{H}}$ we will use path integrals (in so called imaginary time), as in [3, 20, 21], based on Feynman–Kac formula applied to the kernel of the Gibbs density operator and its corresponding Weyl quantization. We start with the kernel representation

$$\left(\mathrm{e}^{-\beta\widehat{H}}\phi\right)(x') = \int_{\mathbb{R}^N} K_\rho(x', y')\phi(y')\,\mathrm{d}y',$$

obtained from that $(\mathrm{e}^{-\beta\widehat{H}}\phi)(x') =: u(x', \beta)$ solves the parabolic partial differential equation

$$\partial_\beta u(\cdot, \beta) + \widehat{H}u(\cdot, \beta) = 0, \quad \beta > 0,\ u(\cdot, 0) = \phi.$$

To motivate the construction of the path integral representation we first identify the Weyl symbol of the density operator in the case of a scalar potential V, *i.e.*, the case $d = 1$. In order to emphasize that we consider the scalar case, we denote this Weyl symbol $\rho_s(x, p)$, and thereby the associated kernel is denoted K_{ρ_s}. Direct application of the Feynman–Kac formula, see Theorem 7.6 in [22], implies that the kernel can be written as the expected value

$$K_{\rho_s}(x', y') = \mathbb{E}\Big[\mathrm{e}^{-\int_0^\beta V(\omega'_r)\,\mathrm{d}r}\delta(\omega'_\beta - y') \,|\, \omega'_0 = x'\Big], \tag{2.13}$$

where ω'_t solves the stochastic differential equation

$$\mathrm{d}\omega'_t = M^{-1/2}\,\mathrm{d}W_t, \qquad \omega'_0 = x',$$

with the standard Wiener process W_t in $\mathbb{R}^N$ and the delta measure $\delta(\omega'_\beta - y')$ concentrated at the point y'.

We recall the definition (2.1) of Weyl quantization for the (scalar) symbol $\rho_s(x, p)$

$$\widehat{\rho}_s\phi(x) = \int_{\mathbb{R}^N} \underbrace{\left(\frac{\sqrt{M}}{2\pi}\right)^N \int_{\mathbb{R}^N} \mathrm{e}^{\mathrm{i}M^{1/2}(x-y)\cdot p}\rho_s(\tfrac{1}{2}(x+y), p)\,\mathrm{d}p}_{=K_{\rho_s}(x,y)}\ \phi(y)\,\mathrm{d}y,$$

from which we obtain the expression for the symbol of an operator associated with the kernel $K_{\rho_s}(x, y)$

$$\rho_s(x, p) = \int_{\mathbb{R}^N} \mathrm{e}^{-\mathrm{i}M^{1/2}y\cdot p} K_{\rho_s}\left(x + \frac{y}{2}, x - \frac{y}{2}\right)\mathrm{d}y. \tag{2.14}$$

Using the substitution $x' = x + \frac{y}{2}$, and $y' = x - \frac{y}{2}$, *i.e.*,

$$y = x' - y' \quad \text{and} \quad x = \frac{x' + y'}{2},$$

and letting

$$\omega'_t = x + \frac{y}{2} - \omega_t$$

where

$$\mathrm{d}\omega_t = M^{-1/2}\,\mathrm{d}W_t, \qquad \omega_0 = 0, \tag{2.15}$$

imply by combining (2.14), (2.13) and the transformed path (2.15)

$$\begin{aligned}\rho_s(x, p) &= \int_{\mathbb{R}^N} \mathrm{e}^{-M^{1/2}\mathrm{i}y\cdot p}\mathbb{E}\Big[\mathrm{e}^{-\int_0^\beta V\left(x+\frac{y}{2}-\omega_r\right)\mathrm{d}r}\delta(y - \omega_\beta) \,|\, \omega_0 = 0\Big]\,\mathrm{d}y \\ &= \mathbb{E}\Big[\mathrm{e}^{-\mathrm{i}M^{1/2}\omega_\beta\cdot p}\mathrm{e}^{-\int_0^\beta V\left(x+\frac{1}{2}\omega_\beta-\omega_r\right)\mathrm{d}r} \,|\, \omega_0 = 0\Big].\end{aligned}$$

We have obtained the path integral representation of the symbol corresponding to the Gibbs density operator $\mathrm{e}^{-\beta\widehat{H}}$ in the case of the scalar potential V

$$\rho_s(x,p) = \mathbb{E}\Big[\mathrm{e}^{-\mathrm{i}W_\beta\cdot p}\mathrm{e}^{-\int_0^\beta V\left(x+M^{-1/2}\left(\frac{1}{2}W_\beta - W_r\right)\right)\mathrm{d}r}\Big], \tag{2.16}$$

as derived in [20].

We can proceed along similar lines in the case of the *matrix-valued* potential V studied here. The Feynman–Kac formula has been derived for operator-valued potentials V, see [21], and in the case where the potential $V(x)$ is a general matrix, the exponential

$$\mathrm{e}^{-\int_0^\beta V\left(x+M^{-1/2}\left(\frac{1}{2}W_\beta - W_r\right)\right)\mathrm{d}r},$$

in (2.16) for the time evolution, is replaced by the corresponding matrix-valued process $\Upsilon_\beta^+ \in \mathbb{R}^{d\times d}$ which solves

$$\dot{\Upsilon}_t^+ = -\Upsilon_t^+ \underbrace{V\Big(x + M^{-1/2}\big(\tfrac{1}{2}W_\beta - W_t\big)\Big)}_{=:V_t^+}, \quad t\in(0,\beta) \text{ and } \Upsilon_0^+ = \mathrm{I}. \tag{2.17}$$

We will use the notation $W_t^\beta := \frac{1}{2}W_\beta - W_t$. The steps in the derivation of (2.16) then imply that the symbol in the case of a matrix-valued potential can again be expressed by

$$\rho(x,p) = \mathbb{E}\Big[\mathrm{e}^{-\mathrm{i}W_\beta\cdot p}\,\Upsilon_\beta^+(W)\,|\,W_0 = 0\Big].$$

To estimate $\rho - \mathrm{e}^{-\beta H}$ we use the symmetry property that the Weyl symbol, ρ, for the Gibbs density operator $\widehat{\rho} = \mathrm{e}^{-\beta\widehat{H}}$ is a Hermitian matrix. Indeed, we have $\mathrm{e}^{-\beta\widehat{H}}$ represented as an L^2-integral operator with the kernel K_ρ and since

$$\widehat{H} = -\frac{1}{2M}\Delta\otimes\mathrm{I} + V(x)$$

is real and Hermitian also $\mathrm{e}^{-\beta\widehat{H}} = \sum_{n=0}^\infty(-\beta\widehat{H})^n/n!$ is real and Hermitian. Therefore the Weyl symbol corresponding to the Gibbs density operator $\widehat{\rho}$ satisfies

$$\rho(x,p) = \int_{\mathbb{R}^N}\mathrm{e}^{-\mathrm{i}M^{1/2}y\cdot p}K_\rho\Big(x+\frac{y}{2},x-\frac{y}{2}\Big)\,\mathrm{d}y = \int_{\mathbb{R}^N}\mathrm{e}^{-\mathrm{i}M^{1/2}y\cdot p}K_\rho\Big(x-\frac{y}{2},x+\frac{y}{2}\Big)\,\mathrm{d}y. \tag{2.18}$$

Either of these integral representations show that ρ is Hermitian. The same steps as above leading to (2.16) can by (2.18) be applied to the change of variables $x' = x - y/2$ and $y' = x + y/2$, which implies that we also have

$$\rho(x,p) = \mathbb{E}\Big[\mathrm{e}^{-\mathrm{i}W_\beta\cdot p}\,\Upsilon_\beta^-(W)\,|\,W_0 = 0\Big],$$

where

$$\dot{\Upsilon}_t^- = -\Upsilon_t^- \underbrace{V\Big(x - M^{-1/2}\big(\tfrac{1}{2}W_\beta - W_t\big)\Big)}_{=:V_t^-}, \quad t\in(0,\beta) \text{ and } \Upsilon_0^- = \mathrm{I}. \tag{2.19}$$

Therefore we have the symmetrized representation

$$\rho(x,p) = \frac{1}{2}\mathbb{E}\Big[\mathrm{e}^{-\mathrm{i}W_\beta\cdot p}\left(\Upsilon_\beta^+(W) + \Upsilon_\beta^-(W)\right)|\,W_0 = 0\Big]. \tag{2.20}$$

Using the path-integral representation of the symbol $\rho(x,p)$ we prove in Section 4.2.

Lemma 2.3. *Assume that the bounds in Theorem 2.1 hold. Then*

$$\begin{aligned}
&\lim_{M\to\infty} M\big(\rho(x,p)-\mathrm{e}^{-\beta H}(x,p)\big)\\
&\quad=\mathrm{e}^{-\beta|p|^2/2}\bigg(\int_0^\beta\Big(\frac{\beta}{2}-t\Big)^2\mathrm{e}^{-tV(x)}p^TV''(x)p\,\mathrm{e}^{-(\beta-t)V(x)}\,\mathrm{d}t\\
&\qquad+\int_0^\beta\int_0^t\Big(\frac{\beta}{2}-s\Big)\Big(\frac{\beta}{2}-t\Big)\mathrm{e}^{-sV(x)}V'(x)p\mathrm{e}^{-(t-s)V(x)}V'(x)p\mathrm{e}^{-(\beta-t)V(x)}\,\mathrm{d}s\,\mathrm{d}t\bigg),
\end{aligned}\tag{2.21}$$

and

$$\begin{aligned}
\|\mathrm{Tr}\,\rho^2\|_{L^\infty(\mathbb{R}^{2N})}&=\mathcal{O}(1),\\
\|\mathrm{Tr}\,\rho^2\|_{L^2(\mathbb{R}^{2N})}&<\infty.
\end{aligned}\tag{2.22}$$

3. Proof of Theorem 2.1

The section proves Theorem 2.1 based on three steps:

Step 1. Use Duhamel's principle recursively to analyse the dynamics based on H,
Step 2. Use estimates of remainders for Weyl compositions and the Weyl Gibbs density to analyse the statistics at $t=0$,
Step 3. Repeat Step 1 and Step 2 with H replaced by $\bar{H}:=\Psi^*\#H\#\Psi$ to approximately diagonalize H.

Proof of the theorem. **Step 1.** Lemma 3.2 shows that the commutator has the representation

$$\mathrm{i}M^{1/2}\Big[\widehat{H},\widehat{a}_s\Big]=\widehat{(\{H,a_s\}+r_s^a)},\tag{3.1}$$

where the remainder r^a vanishes as $M\to\infty$. By Duhamel's principle we have by (2.6) and (2.7) as in (2.10)

$$\begin{aligned}
\mathrm{Tr}\left(\widehat{A}_t\widehat{B}_0\mathrm{e}^{-\beta\widehat{H}}-\widehat{a}_t\widehat{B}_0\mathrm{e}^{-\beta\widehat{H}}\right)&=\int_0^t\mathrm{Tr}\left(\mathrm{e}^{\mathrm{i}M^{1/2}(t-s)\widehat{H}}\left(\mathrm{i}M^{1/2}\Big[\widehat{H},\widehat{a}_s\Big]-\widehat{\{h,a_s\}}\right)\mathrm{e}^{-\mathrm{i}M^{1/2}(t-s)\widehat{H}}\widehat{B}_0\mathrm{e}^{-\beta\widehat{H}}\right)\mathrm{d}s\\
&=\int_0^t\mathrm{Tr}\left(\mathrm{e}^{\mathrm{i}M^{1/2}(t-s)\widehat{H}}\underbrace{\left(\widehat{\{H,a_s\}}+\hat{r}^a-\widehat{\{h,a_s\}}\right)}_{=:\widehat{Da_s}}\mathrm{e}^{-\mathrm{i}M^{1/2}(t-s)\widehat{H}}\widehat{B}_0\mathrm{e}^{-\beta\widehat{H}}\right)\mathrm{d}s
\end{aligned}\tag{3.2}$$

and the cyclic invariance of the trace together with $[\mathrm{e}^{\mathrm{i}M^{1/2}(t-s)\widehat{H}},\mathrm{e}^{-\beta\widehat{H}}]=0$ imply

$$\begin{aligned}
\mathrm{Tr}\left(\widehat{A}_t\widehat{B}_0\mathrm{e}^{-\beta\widehat{H}}-\widehat{a}_t\widehat{B}_0\mathrm{e}^{-\beta\widehat{H}}\right)&=\int_0^t\mathrm{Tr}\left(\widehat{Da_s}\mathrm{e}^{-\mathrm{i}M^{1/2}(t-s)\widehat{H}}\widehat{B}_0\mathrm{e}^{\mathrm{i}M^{1/2}(t-s)\widehat{H}}\mathrm{e}^{-\beta\widehat{H}}\right)\mathrm{d}s\\
&=\int_0^t\mathrm{Tr}\left(\widehat{Da_s}\widehat{B}_{s-t}\mathrm{e}^{-\beta\widehat{H}}\right)\mathrm{d}s.
\end{aligned}\tag{3.3}$$

The right hand side can again be estimated by applying Duhamel's principle (3.3), now to $\widehat{B}_{s-t}$ and b_{s-t}, as follows

$$\int_0^t\mathrm{Tr}\left(\widehat{Da_s}\widehat{B}_{s-t}\mathrm{e}^{-\beta\widehat{H}}\right)\mathrm{d}s-\underbrace{\int_0^t\mathrm{Tr}\left(\widehat{Da_s}\widehat{b}_{s-t}\mathrm{e}^{-\beta\widehat{H}}\right)\mathrm{d}s}_{=:T_0}$$

$$= \int_0^t \int_0^{s-t} \operatorname{Tr}\left(\mathrm{e}^{-\beta\widehat{H}}\widehat{Da_s}\mathrm{e}^{\mathrm{i}M^{1/2}(s-t-\tau)\widehat{H}}\widehat{Db_\tau}\mathrm{e}^{-\mathrm{i}M^{1/2}(s-t-\tau)\widehat{H}}\right)\mathrm{d}\tau\,\mathrm{d}s =: T_3. \tag{3.4}$$

We have by Cauchy's inequality and the cyclic invariance of the trace

$$\begin{aligned}|T_3| &\le \int_0^t \int_0^{t-s} \left(\operatorname{Tr}\left(\left(\widehat{Da_s}\right)^*\widehat{Da_s}\mathrm{e}^{-\beta\widehat{H}}\right)\times \operatorname{Tr}\left(\left(\mathrm{e}^{\mathrm{i}M^{1/2}(s-t-\tau)\widehat{H}}\widehat{Db_\tau}\mathrm{e}^{-\beta\widehat{H}/2}\mathrm{e}^{-\mathrm{i}M^{1/2}(s-t-\tau)\widehat{H}}\right)^*\right.\right.\\ &\quad\left.\left.\times\left(\mathrm{e}^{\mathrm{i}M^{1/2}(s-t-\tau)\widehat{H}}\widehat{Db_\tau}\mathrm{e}^{-\beta\widehat{H}/2}\mathrm{e}^{-\mathrm{i}M^{1/2}(s-t-\tau)\widehat{H}}\right)\right)\right)^{1/2}\mathrm{d}\tau\,\mathrm{d}s\\ &= \int_0^t \int_0^{t-s} \left(\operatorname{Tr}\left(\left(\widehat{Da_s}\right)^*\widehat{Da_s}\mathrm{e}^{-\beta\widehat{H}}\right)\operatorname{Tr}\left(\left(\widehat{Db_\tau}\right)^*\widehat{Db_\tau}\mathrm{e}^{-\beta\widehat{H}}\right)\right)^{1/2}\mathrm{d}\tau\,\mathrm{d}s.\end{aligned} \tag{3.5}$$

The following two lemmas, proved in Section 4, estimate the remainder terms T_0 and T_3.

Lemma 3.1 (Mean-field approximation)**.** *Assume that the bounds in Theorem 2.1 hold, then*

$$\frac{|T_0|}{\operatorname{Tr}\left(\mathrm{e}^{-\beta\widehat{H}}\right)} = \mathcal{O}\big(t\epsilon_1^2 + tM^{-1}\big). \tag{3.6}$$

Lemma 3.2 (Composition analysis)**.** *Assume that the bounds in Theorem 2.1 hold and that c and d are in the Schwartz space $\mathcal{S}$, then*

$$\begin{aligned}c\#d &= cd + \mathfrak{r}_{cd},\\ \lim_{M\to\infty} M^{1/2}\mathfrak{r}_{cd} &= \frac{\mathrm{i}}{2}(\nabla_z\cdot\nabla'_{z'})c(z)d(z')\big|_{z=z'},\end{aligned}$$

and if c and d are scalar valued

$$\begin{aligned}\frac{1}{2}(c\#d + d\#c) &= cd + r_{cd},\\ \lim_{M\to\infty} Mr_{cd} &= \frac{1}{8}(\nabla_z\cdot\nabla'_{z'})^2c(z)d(z')\big|_{z=z'},\end{aligned}$$

and if c is scalar valued

$$\begin{aligned}\mathrm{i}M^{1/2}(H\#c - c\#H) &= \{H,c\} + r_c,\\ r_c &= \frac{1}{8M}\int_0^1 \cos\Big(\frac{\bar{s}}{2M^{1/2}}\nabla_z\cdot\nabla'_{z'}\Big)(\nabla_z\cdot\nabla'_{z'})^3H(z)c(z')\big|_{z=z'}(1-\bar{s})^2\,\mathrm{d}\bar{s},\\ \lim_{M\to\infty} Mr_c &= \frac{1}{24}(\nabla_z\cdot\nabla'_{z'})^3H(z)c(z')\big|_{z=z'},\end{aligned}$$

where the limits hold in $L^1(\mathbb{R}^{2N})$ and $L^\infty(\mathbb{R}^{2N})$. Furthermore the function $a_t:\mathbb{R}^{2N}\to\mathbb{C}$, defined in (2.5), is in the Schwartz class and there holds

$$\frac{|T_3|}{\operatorname{Tr}\left(\mathrm{e}^{-\beta\widehat{H}}\right)} = \mathcal{O}\big(t^2\big(\epsilon_2^2 + M^{-1}\big)\big).$$

The combination of (3.2)–(3.5), Lemmas 3.1 and 3.2 imply

$$\frac{\left|\operatorname{Tr}\left(\widehat{A}_t\widehat{B}_0\mathrm{e}^{-\beta\widehat{H}} - \widehat{a}_t\widehat{B}_0\mathrm{e}^{-\beta\widehat{H}}\right)\right|}{\operatorname{Tr}\left(\mathrm{e}^{-\beta\widehat{H}}\right)} = \mathcal{O}\big(tM^{-1} + t\epsilon_1^2 + t^2\epsilon_2^2\big). \tag{3.7}$$

Similarly the symmetrized difference has the same bound

$$\begin{aligned}&\operatorname{Tr}\left(\left(\widehat{A}_t\widehat{B}_0+\widehat{B}_0\widehat{A}_t\right)\mathrm{e}^{-\beta\widehat{H}}\right)-\operatorname{Tr}\left((\widehat{a}_t\widehat{B}_0+\widehat{B}_0\widehat{a}_t)\mathrm{e}^{-\beta\widehat{H}}\right)\\&\quad=\operatorname{Tr}\left(\left(\widehat{A}_t\widehat{b}_0+\widehat{b}_0\widehat{A}_t\right)\mathrm{e}^{-\beta\widehat{H}}\right)-\operatorname{Tr}\left(\left(\widehat{a}_t\widehat{b}_0+\widehat{b}_0\widehat{a}_t\right)\mathrm{e}^{-\beta\widehat{H}}\right)=\mathcal{O}\big(tM^{-1}+t\epsilon_1^2+t^2\epsilon_2^2\big)\operatorname{Tr}\left(\mathrm{e}^{-\beta\widehat{H}}\right),\end{aligned}\tag{3.8}$$

obtained by interchanging the role of $\widehat{A}$ and $\widehat{B}$ in (3.7).

Step 2. Here we estimate the second term in the left hand side of (3.8), which can be split into

$$\operatorname{Tr}\left(\left(\widehat{a}_t\widehat{b}_0+\widehat{b}_0\widehat{a}_t\right)\mathrm{e}^{-\beta\widehat{H}}\right)=\operatorname{Tr}\left(\left(\widehat{a}_t\widehat{b}_0+\widehat{b}_0\widehat{a}_t\right)\widehat{\mathrm{e}^{-\beta H}}\right)+\operatorname{Tr}\left(\left(\widehat{a}_t\widehat{b}_0+\widehat{b}_0\widehat{a}_t\right)\left(\mathrm{e}^{-\beta\widehat{H}}-\widehat{\mathrm{e}^{-\beta H}}\right)\right).\tag{3.9}$$

The first term in the right hand side in (3.9) has by Lemma 2.2 the classical molecular dynamics approximation

$$\begin{aligned}\operatorname{Tr}\left(\frac{\widehat{a}_t\widehat{b}_0+\widehat{b}_0\widehat{a}_t}{2}\widehat{\mathrm{e}^{-\beta H}}\right)&=\left(\frac{\sqrt{M}}{2\pi}\right)^N\int_{\mathbb{R}^{2N}}\operatorname{Tr}\left(\frac{(a_t\#b_0+b_0\#a_t)(x,p)}{2}\mathrm{e}^{-\beta H(x,p)}\right)\mathrm{d}x\,\mathrm{d}p\\&=\left(\frac{\sqrt{M}}{2\pi}\right)^N\int_{\mathbb{R}^{2N}}\operatorname{Tr}\left(a_0(z_t(z_0))b_0(z_0)\mathrm{e}^{-\beta H(z_0)}\right)+\operatorname{Tr}\left(r_{ab}(z_0)\mathrm{e}^{-\beta H(z_0)}\right)\mathrm{d}z_0,\end{aligned}\tag{3.10}$$

where by Lemma 3.2

$$\lim_{M\to\infty}M\int_{\mathbb{R}^{2N}}\operatorname{Tr}\left(r_{ab}(z_0)\mathrm{e}^{-\beta H(z_0)}\right)\mathrm{d}z_0=\frac{1}{16}\int_{\mathbb{R}^{2N}}\operatorname{Tr}\left(\mathrm{e}^{-\beta H(z_0)}\right)\left(\nabla_{z_0}\cdot\nabla'_{z'_0}\right)^2(a_0(z_t(z_0))b_0(z'_0))\big|_{z_0=z'_0}\,\mathrm{d}z_0.\tag{3.11}$$

It remains to estimate the second term in the right hand side of (3.9). We have

$$\operatorname{Tr}\left(\frac{\widehat{a}_t\widehat{b}_0+\widehat{b}_0\widehat{a}_t}{2}\left(\widehat{\mathrm{e}^{-\beta H}}-\widehat{\rho}\right)\right)=\left(\frac{\sqrt{M}}{2\pi}\right)^N\int_{\mathbb{R}^{2N}}\operatorname{Tr}\left(\frac{a_t\#b_0+b_0\#a_t}{2}\left(\mathrm{e}^{-\beta H}-\rho\right)\right)\mathrm{d}z$$

and Lemmas 2.3 and 3.2 imply

$$\begin{aligned}&\lim_{M\to\infty}\left(M\int_{\mathbb{R}^{2N}}\operatorname{Tr}\left(\frac{a_t\#b_0+b_0\#a_t}{2}\left(\mathrm{e}^{-\beta H}-\rho\right)\right)\mathrm{d}z\right)\\&\quad=\int_{\mathbb{R}^{2N}}\operatorname{Tr}\left(2^{-1}(a_tb_0+b_0a_t)(x,p)\mathrm{e}^{-\beta|p|^2/2}\int_0^\beta\left(\frac{\beta}{2}-r\right)^2\mathrm{e}^{-rV(x)}p^TV''(x)p\mathrm{e}^{-(\beta-r)V(x)}\,\mathrm{d}r\right)\mathrm{d}x\,\mathrm{d}p\\&\qquad+\int_{\mathbb{R}^{2N}}\operatorname{Tr}\left(2^{-1}(a_tb_0+b_0a_t)(x,p)\mathrm{e}^{-\beta|p|^2/2}\right.\\&\qquad\left.\times\int_0^\beta\int_0^r\left(\frac{\beta}{2}-s\right)\left(\frac{\beta}{2}-r\right)\mathrm{e}^{-sV(x)}V'(x)pe^{-(r-s)V(x)}V'(x)p\mathrm{e}^{-(\beta-r)V(x)}\,\mathrm{d}s\,\mathrm{d}r\right)\mathrm{d}x\,\mathrm{d}p\\&\quad=\frac{\beta^3}{24}\int_{\mathbb{R}^{2N}}(a_tb_0+b_0a_t)(x,p)\mathrm{e}^{-\beta|p|^2/2}\operatorname{Tr}\left(p^TV''(x)p\mathrm{e}^{-\beta V(x)}\right)\mathrm{d}x\,\mathrm{d}p+\mathcal{O}(1)\\&\quad=\mathcal{O}(1),\end{aligned}\tag{3.12}$$

where the second last equality follows by interchanging the order of the trace and the integration with respect to β and using the cyclic invariance of the trace. The first equality is obtained by splitting the integral as

$$\int_{\mathbb{R}^{2N}}\ldots=\int_{\mathbb{L}_m^c}\ldots+\int_{\mathbb{L}_m}\ldots$$

over a compact set $\mathbb{L}_m^c := \{z \in \mathbb{R}^{2N} \ : \ h(z) \leq m\}$ and its complement $\mathbb{L}_m := \{z \in \mathbb{R}^{2N} \ : \ h(z) > m\}$ and using that ρ is uniformly bounded in $L^\infty(\mathbb{R}^{2N})$: the second integral is zero for m sufficiently large, as verified in (3.14) below, and in the compact set we apply dominated convergence.

Verification of $\int_{\mathbb{L}_m} |a_t(z_0)| \, \mathrm{d}z_0 = 0$. The integration with respect to the initial data measure $\mathrm{d}z_0$ can be replaced by integration with respect to $\mathrm{d}z_t$ since the phase space volume is preserved, *i.e.*, the Jacobian determinant

$$\left| \det \left(\frac{\partial z_0}{\partial z_t} \right) \right| = 1$$

is constant for all time by Liouville's theorem. We first verify that

$$h(z) \to \infty \text{ as } |z| \to \infty. \tag{3.13}$$

By assumption $\int_{\mathbb{R}^N} \operatorname{Tr} \mathrm{e}^{-\beta V(x)} \, \mathrm{d}x < \infty$. Therefore the smallest eigenvalue $\lambda_0(x)$ of $V(x)$ also satisfies $\int_{\mathbb{R}^N} \mathrm{e}^{-\beta \lambda_0(x)} \, \mathrm{d}x < \infty$ and as $h(x,p) \geq |p|^2/2 + \lambda_0(x)$ we have $\int_{\mathbb{R}^{2N}} \mathrm{e}^{-\beta h(x,p)} \, \mathrm{d}x \, \mathrm{d}p < \infty$, which combined with the assumption $\|\nabla_x h(x,p)\|_{L^\infty(\mathbb{R}^{2N})} \leq C$ establishes (3.13). By using the two properties $h(z_t(z_0)) = h(z_0)$ and $h(z) \to \infty$ as $|z| \to \infty$ together with the compact support of a_0 we obtain

$$\begin{aligned} \int_{\mathbb{L}_m} |a_0(z_t(x_0,p_0))| \, \mathrm{d}z_0 &= \int_{\mathbb{L}_m} |a_0(z_t(x_0,p_0))| \left| \det \left(\frac{\partial z_0}{\partial z_t} \right) \right| \mathrm{d}z_t \\ &= \int_{\mathbb{L}_m} |a_0(z)| \, \mathrm{d}z = 0 \text{ as } m \to \infty. \end{aligned} \tag{3.14}$$

In conclusion we have

$$\frac{1}{2} \operatorname{Tr} \left(\left(\widehat{a}_t \widehat{b}_0 + \widehat{b}_0 \widehat{a}_t \right) \mathrm{e}^{-\beta \widehat{H}} \right) = \left(\frac{\sqrt{M}}{2\pi} \right)^N \left(\int_{\mathbb{R}^{2N}} \operatorname{Tr} \left(a_0(z_t(z_0)) b_0(z_0) \mathrm{e}^{-\beta H}(z_0) \right) + \mathcal{O}\left(M^{-1}\right) \right),$$

which combined with (3.8) proves the theorem for $\Psi = \mathrm{I}$.

Step 3. To improve the error estimate ϵ_2^2 we study the transformed Hamiltonian operator

$$\widehat{\bar{H}} := \Psi^* \widehat{H} \Psi$$

where $\Psi : \mathbb{R}^N \to \mathbb{C}^{d \times d}$ and $\Psi(x)$ is any twice differentiable orthogonal matrix with the Hermitian transpose $\Psi^*(x)$. This Step 3 has the three substeps:

Step 3.1. Study the dynamics under $\bar{H}$.
Step 3.2. Analyse $\bar{H} = \Psi^* \# H \# \Psi$.
Step 3.3. Modify Steps 1 and 2.

Step 3.1. Let α be any complex number and define for $t \in \mathbb{R}$ the exponential

$$\widehat{\bar{y}_t} := \Psi^* \mathrm{e}^{t\alpha \hat{H}} \Psi.$$

Differentiation shows that

$$\partial_t \widehat{\bar{y}_t} = \alpha \Psi^* \hat{H} \Psi \Psi^* \mathrm{e}^{t\alpha \hat{H}} \Psi = \alpha \Psi^* \hat{H} \Psi \widehat{\bar{y}_t}$$

and consequently

$$\widehat{\bar{y}_t} = \mathrm{e}^{t\alpha \Psi^* \hat{H} \Psi} = \mathrm{e}^{t\alpha \widehat{\bar{H}}}.$$

Therefore the transformed variable

$$\widehat{\bar{A}(t,z)} := \Psi^* \widehat{A}_t \Psi, \quad t \in \mathbb{R}, \tag{3.15}$$

evolves with the dynamics $\widehat{\bar{H}}$

$$\begin{aligned}\widehat{\bar{A}_t} &= \Psi^* \widehat{A}_t \Psi \\ &= \Psi^* \mathrm{e}^{\mathrm{i}tM^{1/2}\widehat{H}} \widehat{A_0} \mathrm{e}^{-\mathrm{i}tM^{1/2}\widehat{H}} \hat{\Psi} \\ &= \mathrm{e}^{\mathrm{i}tM^{1/2}\widehat{H}} \widehat{\bar{A}_0} \mathrm{e}^{-\mathrm{i}tM^{1/2}\widehat{\bar{H}}}.\end{aligned}$$

and the cyclic property of the trace implies that the quantum observable satisfies

$$\mathrm{Tr}\left(\widehat{A_t}\widehat{B_0}\mathrm{e}^{-\beta\widehat{H}}\right) = \mathrm{Tr}\left(\underbrace{\Psi\Psi^*}_{=\mathrm{I}}\widehat{A_t}\widehat{B_0}\mathrm{e}^{-\beta\widehat{H}}\right) = \mathrm{Tr}\left(\Psi^*\widehat{A_t}\Psi\Psi^*\widehat{B_0}\Psi\Psi^*\mathrm{e}^{-\beta\widehat{H}}\Psi\right) = \mathrm{Tr}\left(\widehat{\bar{A}_t}\widehat{\bar{B}_0}\mathrm{e}^{-\beta\widehat{\bar{H}}}\right), \tag{3.16}$$

where the initial symbols are given by

$$\begin{aligned}\bar{A}_0 &= \Psi^* \# a_0 \# \Psi, \\ \bar{B}_0 &= \Psi^* \# b_0 \# \Psi.\end{aligned}$$

Step 3.2. We have

$$\bar{H}(x,p) = \Psi^* \# H \# \Psi(x,p) = \Psi^*(x) H(x,p) \Psi(x) + \frac{1}{4M} \nabla\Psi^*(x) \cdot \nabla\Psi(x), \tag{3.17}$$

as derived in [2] from the composition in (2.12):

$$\begin{aligned}\Psi^* \# H \# \Psi(x,p) &= \Psi^*(x) \# \left(H(x,p)\Psi(x) + \frac{\mathrm{i}M^{-1/2}}{2} p \cdot \nabla\Psi(x) - \frac{M^{-1}}{4}\Delta\Psi(x)\right) \\ &= \Psi^*(x) H(x,p) \Psi(x) + \frac{\mathrm{i}M^{-1/2}}{2} p \cdot \nabla\Psi^*(x)\Psi(x) - \frac{M^{-1}}{4}\Delta\Psi^*(x)\Psi(x) \\ &\quad + \frac{\mathrm{i}}{2M^{1/2}} \Psi^*(x) p \cdot \nabla\Psi(x) - \frac{1}{4M}\nabla\Psi^*(x)\cdot\nabla\Psi(x) - \frac{1}{4M}\Psi^*(x)\Delta\Psi(x)\end{aligned}$$

where by the orthogonality $\Psi^*\Psi = \mathrm{I}$

$$\begin{aligned}\Psi^* \# H \# \Psi(x,p) &= \Psi^*(x) H(x,p)\Psi(x) + \frac{\mathrm{i}}{2M^{1/2}} p \cdot \nabla(\Psi^*(x)\Psi(x)) \\ &\quad - \frac{1}{4M}(\Delta(\Psi^*(x)\Psi(x)) - \nabla\Psi^*(x)\cdot\nabla\Psi(x)) \\ &= \Psi^*(x) H(x,p)\Psi(x) + \frac{1}{4M}\nabla\Psi^*(x)\cdot\nabla\Psi(x).\end{aligned}$$

Let $\Psi(x)$ be the orthogonal matrix composed of the eigenvectors to $V(x)$, then the matrix

$$\Psi^*(x) H(x,p) \Psi(x) = \frac{|p|^2}{2}\mathrm{I} + \Lambda(x)$$

is diagonal, with the eigenvectors $\lambda_i(x)$ of $V(x)$ forming the diagonal $d \times d$ matrix $\Lambda(x)$. The non diagonal part $\frac{1}{4M}\nabla\Psi^*(x)\cdot\nabla\Psi(x)$ of $\bar{H}(x,p)$ is small if $\Psi(x)$ is differentiable everywhere. If the eigenvectors to V are not differentiable in a point x_*, we may use a regularized version of Ψ in a neighbourhood of x_* to form an approximate diagonalization of H.

Step 3.3. The derivation in Step 1 can now be repeated with H replaced by $\bar{H}$ and A, B by $\bar{A}, \bar{B}$. Duhamel's principle (2.10) implies

$$\widehat{\bar{A}_t} - \widehat{a_t} - \left(\widehat{\bar{A}_0} - \widehat{a_0}\right) = \int_0^t \mathrm{e}^{\mathrm{i}M^{1/2}(t-s)\widehat{\bar{H}}} \left(\mathrm{i}M^{1/2}\left[\widehat{\bar{H}}, \widehat{a_s}\right] - \widehat{\{h, a_s\}}\right) \mathrm{e}^{-\mathrm{i}M^{1/2}(t-s)\widehat{\bar{H}}}\,\mathrm{d}s,$$

and we obtain by (3.16) as in (3.7)

$$\begin{aligned}\operatorname{Tr}\left(\widehat{A}_t\widehat{B}_0\mathrm{e}^{-\beta\widehat{H}}-\widehat{a}_t\widehat{\bar{B}}_0\mathrm{e}^{-\beta\widehat{\bar{H}}}\right)&=\operatorname{Tr}\left(\widehat{\bar{A}}_t\widehat{\bar{B}}_0\mathrm{e}^{-\beta\widehat{\bar{H}}}-\widehat{a}_t\widehat{\bar{B}}_0\mathrm{e}^{-\beta\widehat{\bar{H}}}\right)\\&=T_0+T_3+\operatorname{Tr}\left(\left(\widehat{\bar{A}_0}-\widehat{a_0}\right)\widehat{\bar{B}}_0\mathrm{e}^{-\beta\widehat{\bar{H}}}\right)+\int_0^t\operatorname{Tr}\left(\widehat{Da_s}\left(\widehat{\bar{B}_0}-\widehat{b_0}\right)\mathrm{e}^{-\beta\widehat{\bar{H}}}\right)\mathrm{d}s,\end{aligned}$$

where H is replaced by $\bar{H}$ in $\widehat{Da}$, $\widehat{Db}$, T_0 and T_3, so that

$$\begin{aligned}T_0&=\int_0^t\operatorname{Tr}\left(\underbrace{\widehat{Da_s}}_{=:\{\bar{H}-h,a_s\}\widehat{\ }+\hat{r}^a}\widehat{b}_{s-t}\mathrm{e}^{-\beta\widehat{\bar{H}}}\right)\mathrm{d}s,\\T_3&=\int_0^t\int_0^{s-t}\operatorname{Tr}\left(\mathrm{e}^{-\beta\widehat{\bar{H}}}\widehat{Da_s}\mathrm{e}^{\mathrm{i}M^{1/2}(s-t-\tau)\widehat{\bar{H}}}\widehat{Db_\tau}\mathrm{e}^{-\mathrm{i}M^{1/2}(s-t-\tau)\widehat{\bar{H}}}\right)\mathrm{d}\tau\,\mathrm{d}s.\end{aligned}$$

The two terms T_0 and T_3 have the bounds in Lemmas 3.1 and 3.2 with H replaced by $\bar{H}$. It remains to show that the initial errors satisfy

$$\frac{\operatorname{Tr}\left(\left(\widehat{\bar{A}_0}-\widehat{a_0}\right)\widehat{\bar{B}}_0\mathrm{e}^{-\beta\widehat{\bar{H}}}\right)}{\operatorname{Tr}\left(\mathrm{e}^{-\beta\widehat{\bar{H}}}\right)}+\frac{\int_0^t\operatorname{Tr}\left(\widehat{Da_s}\left(\widehat{\bar{B}_0}-\widehat{b_0}\right)\mathrm{e}^{-\beta\widehat{\bar{H}}}\right)\mathrm{d}s}{\operatorname{Tr}\left(\mathrm{e}^{-\beta\widehat{\bar{H}}}\right)}=\mathcal{O}\big(M^{-1}\big).\tag{3.18}$$

To prove (3.18) let $\widehat{\bar{\rho}}=\mathrm{e}^{-\beta\widehat{\bar{H}}}$, then by the composition (2.12) and Lemma 2.2 we obtain

$$\begin{aligned}\operatorname{Tr}\left(\left(\widehat{\bar{A}_0}-\widehat{a_0}\right)\widehat{\bar{B}}_0\mathrm{e}^{-\beta\widehat{\bar{H}}}\right)&=\operatorname{Tr}\left(\left((\bar{A}_0-a_0)\#\bar{B}_0\right)\widehat{\ }\,\widehat{\bar{\rho}}\right)\\&=\left(\frac{\sqrt{M}}{2\pi}\right)^N\int_{\mathbb{R}^{2N}}\operatorname{Tr}\left(\left((\bar{A}_0-a_0)\#\bar{B}_0\right)\bar{\rho}\right)\mathrm{d}x\,\mathrm{d}p.\end{aligned}$$

To estimate the initial error $\bar{A}_0-a_0$ we use Lemma 3.2

$$\begin{aligned}a_0\#\Psi(x,p)&=a_0(x,p)\Psi(x)+\frac{\mathrm{i}}{2\sqrt{M}}\nabla_p a_0(x,p)\cdot\nabla_x\Psi(x)\\&\quad-\frac{1}{4M}\int_0^1\mathrm{e}^{-\frac{\mathrm{i}s}{2}M^{-1/2}\nabla_x\cdot\nabla_p}(\nabla_x\cdot\nabla_p)^2a_0(x',p)\Psi(x)(1-s)\,\mathrm{d}s\big|_{x'=x},\end{aligned}$$

which by the composition (2.12) implies

$$\begin{aligned}\bar{A}_0(x,p)&=\Psi^*\#a_0\#\Psi(x,p)\\&=\Psi^*(x)(a_0\#\Psi)(x,p)+\frac{\mathrm{i}}{2\sqrt{M}}\nabla_x\Psi^*(x)\cdot\nabla_p(a_0\#\Psi)(x,p)\\&\quad-\frac{1}{4M}\int_0^1\mathrm{e}^{-\frac{\mathrm{i}s}{2}M^{-1/2}\nabla_x\cdot\nabla_p}(\nabla_x\cdot\nabla_p)^2\Psi^*(x)(a_0\#\Psi)(x',p)(1-s)\,\mathrm{d}s\big|_{x'=x}\\&=a_0(x,p)\underbrace{\Psi^*(x)\Psi(x)}_{=\mathrm{I}}+\frac{\mathrm{i}}{2\sqrt{M}}\nabla_p a_0(x,p)\cdot\underbrace{\nabla_x(\Psi^*(x)\Psi(x))}_{=0}\\&\quad-\frac{1}{4M}\Psi^*(x)\int_0^1\mathrm{e}^{-\frac{\mathrm{i}s}{2}M^{-1/2}\nabla_x\cdot\nabla_p}(\nabla_x\cdot\nabla_p)^2(a_0(x',p)\Psi(x))(1-s)\,\mathrm{d}s\big|_{x'=x}\\&\quad-\frac{1}{4M}(\nabla_{x'}\cdot\nabla_p)(\nabla_x\cdot\nabla_p)(\Psi^*(x')a_0(x'',p)\Psi(x))\big|_{x''=x'=x}\end{aligned}$$

$$+\frac{\mathrm{i}}{8M^{3/2}}\int_0^1 \mathrm{e}^{-\frac{\mathrm{i}s}{2}M^{-1/2}\nabla_x\cdot\nabla_p}(\nabla_x\cdot\nabla_p)^2\Psi^*(x)(a_0(x',p)\Psi(x))(1-s)\,\mathrm{d}s\big|_{x'=x}$$
$$-\frac{1}{4M}\int_0^1 \mathrm{e}^{-\frac{\mathrm{i}s}{2}M^{-1/2}\nabla_x\cdot\nabla_p}(\nabla_x\cdot\nabla_p)^2\Psi^*(x)(a_0\#\Psi)(x',p)(1-s)\,\mathrm{d}s\big|_{x'=x}.$$

Here the orthogonality $\Psi^*\Psi=\mathrm{I}$ implies $\nabla(\Psi^*\Psi)=0$. We obtain as in (3.11) the limit

$$\begin{aligned}
&\lim_{M\to\infty} M\int_{\mathbb{R}^{2N}}\mathrm{Tr}\left(\left(\bar{A}_0-a_0\right)\bar{B}_0\bar{\rho}\right)\mathrm{d}x\,\mathrm{d}p\\
&\quad=-\int_{\mathbb{R}^{2N}}\mathrm{Tr}\left(\left[\frac{1}{8}\Psi^*(x)(\nabla_x\cdot\nabla_p)^2a_0(x',p)\Psi(x)\big|_{x'=x}\right.\right.\\
&\qquad+\frac{1}{4}(\nabla_{x'}\cdot\nabla_p)(\nabla_x\cdot\nabla_p)\Psi^*(x')a_0(x'',p)\Psi(x)\big|_{x''=x'=x}\\
&\qquad\left.\left.+\frac{1}{8}(\nabla_x\cdot\nabla_p)^2\Psi^*(x)a_0(x',p)\Psi(x')\big|_{x'=x}\right]b_0(x,p)\mathrm{e}^{-\beta\Psi^*(x)H(x,p)\Psi(x)}\right)\mathrm{d}x\,\mathrm{d}p
\end{aligned}$$

and similarly

$$\int_0^t\mathrm{Tr}\left(\widehat{Da_s}\left(\widehat{\bar{B}_0}-\widehat{b_0}\right)\mathrm{e}^{-\beta\widehat{\bar{H}}}\right)\mathrm{d}s=\left(\frac{\sqrt{M}}{2\pi}\right)^N\int_{\mathbb{R}^{2N}}\mathrm{Tr}\left(\left(Da_s\#\left(\bar{B}_0-b_0\right)\right)\bar{\rho}\right)\mathrm{d}x\,\mathrm{d}p$$

where

$$\begin{aligned}
&\lim_{M\to\infty}\left(M\int_{\mathbb{R}^{2N}}\mathrm{Tr}\left(\left(Da_s\#(\bar{B}_0-b_0)\right)\bar{\rho}\right)\mathrm{d}x\,\mathrm{d}p\right)\\
&\quad=-\int_{\mathbb{R}^{2N}}\mathrm{Tr}\left(\left\{\bar{H}(x,p)-h(x,p),a_s(x,p)\right\}\left[\frac{1}{8}\Psi^*(x)(\nabla_x\cdot\nabla_p)^2b_0(x',p)\Psi(x)\big|_{x'=x}\right.\right.\\
&\qquad+\frac{1}{4}(\nabla_{x'}\cdot\nabla_p)(\nabla_x\cdot\nabla_p)\Psi^*(x')b_0(x'',p)\Psi(x)\big|_{x''=x'=x}\\
&\qquad\left.\left.+\frac{1}{8}(\nabla_x\cdot\nabla_p)^2\Psi^*(x)b_0(x',p)\Psi(x')\big|_{x'=x}\right]\mathrm{e}^{-\beta\Psi^*(x)H(x,p)\Psi(x)}\right)\mathrm{d}x\,\mathrm{d}p.
\end{aligned}$$

which proves (3.18). □

4. Proof of Lemmas

This section estimates the remainder terms T_0 and T_3 and the statistical error $\rho-\mathrm{e}^{-\beta H}$. The error term T_3 in Lemma 3.2 is due to remainders from classical approximation while T_0 in Lemma 3.1 is the main term regarding the mean-field approximation. The statistical error is estimated in Lemma 2.3.

4.1. Proof of Lemma 3.1

Proof. We consider first the case $\Psi=\mathrm{I}$, *i.e.*, $\bar{H}=H$. We have

$$\begin{aligned}
\int_0^t\mathrm{Tr}\left(\widehat{Da_s}\widehat{b}_{s-t}\mathrm{e}^{-\beta\widehat{H}}\right)\mathrm{d}s&=\int_0^t\mathrm{Tr}\left(\left(\widehat{\{H,a_s\}}+\hat{r}_s^a-\widehat{\{h,a_s\}}\right)\widehat{b}_{s-t}\mathrm{e}^{-\beta\widehat{H}}\right)\mathrm{d}s\\
&=\int_0^t\mathrm{Tr}\left(\widehat{\{H-h,a_s\}}\,\widehat{b}_{s-t}\mathrm{e}^{-\beta\widehat{H}}\right)\mathrm{d}s+\int_0^t\mathrm{Tr}\left(\hat{r}_s^a\widehat{b}_{s-t}\mathrm{e}^{-\beta\widehat{H}}\right)\mathrm{d}s
\end{aligned}$$

$$= \left(\frac{M^{1/2}}{2\pi}\right)^N \int_0^t \int_{\mathbb{R}^{2N}} \mathrm{Tr}\left((\{H-h, a_s\}\#b_{s-t})\rho\right) \mathrm{d}z\, \mathrm{d}s \tag{4.1}$$
$$+ \left(\frac{M^{1/2}}{2\pi}\right)^N \int_0^t \int_{\mathbb{R}^{2N}} \mathrm{Tr}\left((r_s^a \# b_{s-t})\rho\right) \mathrm{d}z\, \mathrm{d}s$$

where the trace in the integrals over phase space $\mathbb{R}^{2N}$ is with respect to $d \times d$ matrices. The inner integral in the second term of the right hand side in (4.1) has by Lemmas 2.3 and 3.2 the limit

$$\lim_{M\to\infty} \left(M \int_{\mathbb{R}^{2N}} \mathrm{Tr}\left((r_s^a \# b_{s-t})\rho\right)\right) \mathrm{d}z$$
$$= \frac{1}{24} \int_{\mathbb{R}^{2N}} \mathrm{Tr}\left(\left(\nabla_{z_0'} \cdot \nabla'_{z_0}\right)^3 (H(z_0) a_0(z_s(z_0'))) \big|_{z_0=z_0'} b_0(z_{s-t}(z_0)) \mathrm{e}^{-\beta H(z_0)} \right) \mathrm{d}z_0, \tag{4.2}$$

using splitting of the phase space integral as in (3.12). Similarly we have by Lemmas 2.3 and 3.2 the limit

$$\lim_{M\to\infty} \int_{\mathbb{R}^{2N}} \mathrm{Tr}\left((\{H-h, a_s\}\#b_{s-t})\rho\right) \mathrm{d}z = \int_{\mathbb{R}^{2N}} \mathrm{Tr}\left(\{H-h, a_s\} b_{s-t} \mathrm{e}^{-\beta H}\right) \mathrm{d}z,$$

and integration by parts together with the mean-field definition (1.6) simplify the first term in the right hand side of (4.1) to

$$\begin{aligned}
&\int_{\mathbb{R}^{2N}} \mathrm{Tr}\left(\{H-h, a_s\} b_{s-t} \mathrm{e}^{-\beta H}\right) \mathrm{d}z \\
&= \int_{\mathbb{R}^{2N}} \mathrm{Tr}\left(\nabla'(H-h) \cdot \nabla a_s \; b_{s-t} \mathrm{e}^{-\beta H}\right) \mathrm{d}z \\
&= -\int_{\mathbb{R}^{2N}} \underbrace{\mathrm{Tr}\left((H-h)\mathrm{e}^{-\beta H}\right)}_{=0} \nabla' \cdot (b_{s-t} \nabla a_s)\, \mathrm{d}z \\
&\quad + \int_{\mathbb{R}^{2N}} \mathrm{Tr}\left((H-h) \int_0^\beta \mathrm{e}^{-\tau H} \nabla a_s \cdot \nabla'(H-h) \mathrm{e}^{-(\beta-\tau)H} b_{s-t}\, \mathrm{d}\tau \right) \mathrm{d}z \\
&\quad + \int_{\mathbb{R}^{2N}} \underbrace{\mathrm{Tr}\left((H-h)\mathrm{e}^{-\beta H}\right)}_{=0} \nabla a_s \cdot \nabla' h \; \beta b_{s-t}\, \mathrm{d}z \\
&= \frac{1}{2} \int_{\mathbb{R}^{2N}} \mathrm{Tr}\left(\int_0^\beta \mathrm{e}^{-\tau H} ((H-h) \nabla a_s \cdot \nabla'(H-h) \right. \\
&\quad \left. + \; (\nabla a_s \cdot \nabla'(H-h)(H-h))) \mathrm{e}^{-(\beta-\tau)H} b_{s-t}\, \mathrm{d}\tau \right) \mathrm{d}z \\
&= \frac{\beta}{2} \int_{\mathbb{R}^{2N}} \mathrm{Tr}\left(\nabla'(H-h)^2 \cdot \nabla a_s e^{-\beta H} b_{s-t}\right) \mathrm{d}z \\
&= -\frac{\beta}{2} \int_{\mathbb{R}^{2N}} \mathrm{Tr}\left((H-h)^2 \nabla a_s \cdot \nabla'\left(\mathrm{e}^{-\beta H} b_{s-t}\right)\right) \mathrm{d}z \\
&\quad - \frac{\beta}{2} \int_{\mathbb{R}^{2N}} \mathrm{Tr}\left((H-h)^2 \underbrace{\nabla' \cdot \nabla(a_s)}_{=0} \left(\mathrm{e}^{-\beta H} b_{s-t}\right) \right) \mathrm{d}z \\
&= -\frac{\beta}{2} \int_{\mathbb{R}^{2N}} \mathrm{Tr}\left((H-h)^2 \nabla a_s \cdot \left(\nabla' b_{s-t} \mathrm{e}^{-\beta H} - b_{s-t} \int_0^\beta \mathrm{e}^{-\tau H} \nabla' H \mathrm{e}^{-(\beta-\tau)H}\, \mathrm{d}\tau \right) \right) \mathrm{d}z \\
&= -\frac{\beta}{2} \int_{\mathbb{R}^{2N}} \mathrm{Tr}\left(\mathrm{e}^{-\beta H} (H-h)^2 \nabla a_s \cdot (\nabla' b_{s-t} - \beta b_{s-t} \nabla' H) \right) \mathrm{d}z.
\end{aligned} \tag{4.3}$$

The third equality uses that $(H-h)$ commutes with $\mathrm{e}^{-\beta H}$ and the forth and the last equality is obtained by interchanging the order of the trace and the integral with respect to τ in combination with the cyclic invariance of the trace. Cauchy's inequality, the positive definiteness of $\mathrm{e}^{-\beta H}(H-h)^2$ and $H-h$ depending only on x imply that the right hand side has the bound

$$\begin{aligned}
&\left|\frac{\beta}{2}\int_{\mathbb{R}^{2N}} \mathrm{Tr}\left(\mathrm{e}^{-\beta H}(H-h)^2\nabla a_s\cdot(\nabla' b_{s-t}-\beta b_{s-t}\nabla' H)\right)\mathrm{d}z\right| \\
&\quad\le \frac{\beta}{2}\int_{\mathbb{R}^{2N}}\left(\mathrm{Tr}\left(\left(\mathrm{e}^{-\beta H}(H-h)^2\right)^2\right)\mathrm{Tr}\left(\left(\nabla a_s\cdot(\nabla' b_{s-t}-\beta b_{s-t}\nabla' H)\right)^2\right)\right)^{1/2}\mathrm{d}z \\
&\quad\le \frac{\beta}{2}\int_{\mathbb{R}^{2N}} \mathrm{Tr}\left(\mathrm{e}^{-\beta V}(H-h)^2\right)\mathrm{e}^{-\beta|p|^2/2}\left(\mathrm{Tr}\left(\left(\nabla a_s\cdot(\nabla' b_{s-t}-\beta b_{s-t}\nabla' H)\right)^2\right)\right)^{1/2}\mathrm{d}z \\
&\quad\le K\int_{\mathbb{R}^N}\mathrm{Tr}\left(\mathrm{e}^{-\beta V}(H-h)^2\right)\mathrm{d}x
\end{aligned} \tag{4.4}$$

for a positive constant K. The combination of (4.2)-(4.4) implies (3.6) and we note that the exponential form $\mathrm{e}^{-\beta H}$ of the Gibbs density was crucial to obtain (4.3).

In the case that $\Psi\neq \mathrm{I}$ we have by (3.17) $\bar{H}=\Psi^* H\Psi+\frac{1}{4M}\nabla\Psi^*\cdot\nabla\Psi$ and the factor $\mathrm{Tr}\left((H-h)\mathrm{e}^{-\beta H}\right)=0$ in (4.3) is replaced by $\mathrm{Tr}\left((\bar{H}-h)\mathrm{e}^{-\beta\bar{H}}\right)$ where

$$\lim_{M\to\infty}\left(M\mathrm{Tr}\left((\bar{H}-h)\mathrm{e}^{-\beta\bar{H}}\right)\right)=\mathrm{Tr}\left(\nabla\Psi^*\cdot\nabla\Psi\mathrm{e}^{-\beta\Psi^* H\Psi}\right).$$

which as in (4.3) and (4.4) imply

$$|T_0|\le\mathcal{O}\big(tM^{-1}+t\epsilon_1^2\big).$$

□

4.2. Proof of Lemma 2.3

Proof. To estimate the difference of the symbols for the Gibbs density, $\rho-\mathrm{e}^{-\beta H}$, we define the solution operator

$$\dot{Y}_t(x)=-Y_t(x)V(x),\qquad Y_0=\mathrm{I}$$

satisfying $Y_t=\mathrm{e}^{-tV}$, which implies $\mathrm{e}^{-\beta H(x,p)}=\mathrm{e}^{-\beta(|p|^2/2+V(x))}=\mathrm{e}^{-\beta|p|^2/2}Y_\beta(x)$. We have by Duhamel's principle

$$\Upsilon_\beta^\pm-Y_\beta=\int_0^\beta\Upsilon_t^\pm\,(V-V_t^\pm)\mathrm{e}^{-(\beta-t)V}\,\mathrm{d}t, \tag{4.5}$$

which by dominated convergence implies

$$\begin{aligned}
\lim_{M\to\infty}M^{1/2}\big(\Upsilon_t^\pm-Y_t\big)&=\lim_{M\to\infty}M^{1/2}\int_0^t\Upsilon_s^\pm\big(V-V_s^\pm\big)\mathrm{e}^{-(t-s)V}\,\mathrm{d}s \\
&=\mp\int_0^t e^{-sV(x)}V'(x)W_s^\beta\mathrm{e}^{-(t-s)V(x)}\,\mathrm{d}s.
\end{aligned} \tag{4.6}$$

The symmetrized relation (2.20) yields

$$\rho-\mathrm{e}^{-\beta H}=\frac{1}{2}\mathbb{E}\Big[\mathrm{e}^{-\mathrm{i}W_\beta\cdot p}\Big(\Big(\Upsilon_\beta^+-Y_\beta\Big)+\Big(\Upsilon_\beta^--Y_\beta\Big)\Big)\Big]$$

which by (4.5), (4.6) and dominated convergence establish

$$\begin{aligned}
&\lim_{M\to\infty}\Big(M\Big(\rho(x,p)-\mathrm{e}^{-\beta H(x,p)}\Big)\Big)\\
&\quad=\frac{1}{2}\mathbb{E}\bigg[\mathrm{e}^{-\mathrm{i}W_\beta\cdot p}\int_0^\beta \lim_{M\to\infty}\big(\Upsilon_t^+M\big(V-V_t^+\big)+\Upsilon_t^-M\big(V-V_t^-\big)\big)\mathrm{e}^{-(\beta-t)V}\,\mathrm{d}t\bigg]\\
&\quad=\mathbb{E}\bigg[\mathrm{e}^{-\mathrm{i}W_\beta\cdot p}\bigg(\frac{1}{2}\int_0^\beta \lim_{M\to\infty}\Big(\big(\Upsilon_t^+-\Upsilon_t^-\big)M^{1/2}\Big)V'(x)W_t^\beta\mathrm{e}^{-(\beta-t)V}\,\mathrm{d}t\\
&\qquad+\frac{1}{4}\int_0^\beta \lim_{M\to\infty}\bigg(\Upsilon_t^+(W_t^\beta)^T\int_0^1 V''\Big(x+sM^{-1/2}W_t^\beta\Big)\,\mathrm{d}sW_t^\beta\mathrm{e}^{-(\beta-t)V}\,\mathrm{d}t\\
&\qquad+\frac{1}{4}\int_0^\beta \lim_{M\to\infty}\bigg(\Upsilon_t^-(W_t^\beta)^T\int_0^1 V''\Big(x-sM^{-1/2}W_t^\beta\Big)\,\mathrm{d}sW_t^\beta\bigg)\mathrm{e}^{-(\beta-t)V}\,\mathrm{d}t\bigg)\bigg)\bigg]\\
&\quad=\mathbb{E}\bigg[\mathrm{e}^{-\mathrm{i}W_\beta\cdot p}\int_0^\beta\int_0^t \mathrm{e}^{-sV}V'(x)W_s^\beta\mathrm{e}^{-(t-s)V}V'(x)W_t^\beta\mathrm{e}^{-(\beta-t)V}\,\mathrm{d}s\,\mathrm{d}t\bigg]\\
&\qquad+\frac{1}{2}\mathbb{E}\bigg[\mathrm{e}^{-\mathrm{i}W_\beta\cdot p}\int_0^\beta \mathrm{e}^{-tV}(W_t^\beta)^TV''(x)W_t^\beta\mathrm{e}^{-(\beta-t)V}\,\mathrm{d}t\bigg].
\end{aligned}\tag{4.7}$$

To determine the path integrals in the right hand side of (4.7) we make a partition of $[0,\beta]$ into time intervals $[t_j,t_{j+1})$, where $t_j=j\beta/J$ for $j=0,\dots,J$ and corresponding Wiener increments $\Delta W_j=W(t_{j+1})-W(t_j)$ and time steps $\Delta t:=\beta/J$, to obtain

$$W_{t_k}^\beta\equiv\frac{1}{2}W_\beta-W_{t_k}=\sum_{j=0}^{J-1}\frac{1}{2}\Delta W_j-\sum_{j<k}\Delta W_j=\sum_{j=0}^{J-1}S_{j,k}\Delta W_j$$

where

$$S_{j,k}:=\begin{cases}\frac{1}{2} & \text{if } j\geq k,\\ -\frac{1}{2} & \text{if } j<k.\end{cases}$$

This partition implies

$$\begin{aligned}
&-\mathbb{E}\bigg[\mathrm{e}^{-\mathrm{i}W_\beta\cdot p}\int_0^\beta \mathrm{e}^{-tV}(W_t^\beta)^TV''(x)W_t^\beta\,\mathrm{e}^{-(\beta-t)V}\,\mathrm{d}t\bigg]\\
&\quad=-\lim_{J\to\infty}\mathbb{E}\bigg[\mathrm{e}^{-\mathrm{i}\sum_{m=0}^{J-1}\Delta W_m\cdot p}\sum_{k=0}^{J-1}\sum_{j=0}^{J-1}\sum_{\ell=0}^{J-1}S_{j,k}S_{\ell,k}\Delta W_j^T\underbrace{\Big(\mathrm{e}^{-k\Delta tV}V''\mathrm{e}^{-(J-k)\Delta tV}\Big)}_{=:V_k''}\Delta W_\ell\Delta t\bigg]\\
&\quad=-\lim_{J\to\infty}\sum_{k=0}^{J-1}\sum_{j=0}^{J-1}\sum_{\ell=0}^{J-1}\Delta tS_{j,k}S_{\ell,k}\times\int_{\mathbb{R}^{NJ}}\mathrm{e}^{-\mathrm{i}\sum_{m=0}^{J-1}\Delta W_m\cdot p}\Delta W_j^TV_k''\Delta W_\ell\prod_{n=0}^{J-1}\frac{\mathrm{e}^{-|\Delta W_n|^2/(2\Delta t)}}{(2\pi\Delta t)^{N/2}}\,\mathrm{d}(\Delta W_n)\\
&\quad=\lim_{J\to\infty}\mathrm{e}^{-J|p|^2\Delta t/2}\sum_{k=0}^{J-1}\Big(\frac{J}{2}-k\Big)^2\Delta t^2p^TV_k''p\,\Delta t\\
&\quad=\mathrm{e}^{-\beta|p|^2/2}\int_0^\beta\Big(\frac{\beta}{2}-t\Big)^2\mathrm{e}^{-tV(x)}p^TV''(x)p\,\mathrm{e}^{-(\beta-t)V(x)}\,\mathrm{d}t=\mathcal{O}(1).
\end{aligned}\tag{4.8}$$

Similarly we have

$$
\begin{aligned}
&-\mathbb{E}\left[\mathrm{e}^{-\mathrm{i}W_\beta\cdot p}\int_0^\beta\int_0^t \mathrm{e}^{-sV}V'(x)W_s^\beta \mathrm{e}^{-(t-s)V}V'(x)W_t^\beta \mathrm{e}^{-(\beta-t)V}\,\mathrm{d}s\,\mathrm{d}t\right]\\
&\quad=-\lim_{J\to\infty}\sum_{k=0}^{J-1}\sum_{r=0}^{J-1}\sum_{j=0}^{J-1}\sum_{\ell=0}^{J-1} S_{j,r}S_{\ell,k}(\Delta t)^2\mathrm{e}^{-\mathrm{i}\sum_{m=0}^{J-1}\Delta W_m\cdot p}\\
&\qquad\times \mathrm{e}^{-r\Delta tV}V'\Delta W_j\mathrm{e}^{(k-r)\Delta tV}V'\Delta W_\ell\mathrm{e}^{-(J-k)\Delta tV}\prod_{n=0}^{J-1}\frac{\mathrm{e}^{-|\Delta W_n|^2/(2\Delta t)}}{(2\pi\Delta t)^{N/2}}\,\mathrm{d}(\Delta W_n)\\
&\quad=\lim_{J\to\infty}\sum_{k=0}^{J-1}\sum_{r=0}^{J-1}(\Delta t)^4\left(\frac{J}{2}-r\right)\left(\frac{J}{2}-k\right)\mathrm{e}^{-J\Delta t|p|^2/2}\mathrm{e}^{-r\Delta tV}V'pe^{-(k-r)\Delta tV}V'p\mathrm{e}^{-(J-k)\Delta tV}\\
&\quad=\mathrm{e}^{-\beta|p|^2/2}\int_0^\beta\int_0^t\left(\frac{\beta}{2}-s\right)\left(\frac{\beta}{2}-t\right)\mathrm{e}^{-sV(x)}V'(x)pe^{-(t-s)V(x)}V'(x)p\mathrm{e}^{-(\beta-t)V(x)}\,\mathrm{d}s\,\mathrm{d}t
\end{aligned}
$$

so that $(\rho-\mathrm{e}^{-\beta H})=\mathcal{O}\big(M^{-1}\big)$.

The construction (2.17) implies

$$
\frac{\mathrm{d}}{\mathrm{d}t}\mathrm{Tr}\left(\left(\Upsilon_t^+\right)^2\right)=\mathrm{Tr}\left(\Upsilon_t^+\left(-2V\left(x+M^{-1/2}W_t^\beta\right)\right)\Upsilon_t^+\right)
$$

and by assumption there is a constant k such that $V+k\mathrm{I}$ is positive definite everywhere. Therefore we have

$$
\frac{\mathrm{d}}{\mathrm{d}t}\mathrm{Tr}\left(\left(\Upsilon_t^+\right)^2\right)\le k\mathrm{Tr}\left(\left(\Upsilon_t^+\right)^2\right)
$$

which establishes $\mathrm{Tr}\,((\Upsilon_\beta^+)^2)\le \mathrm{e}^{k\beta}$ and shows that for independent Wiener processes W and W' we obtain by Cauchy's inequality

$$
\begin{aligned}
\mathrm{Tr}\,\rho^2&=\mathrm{Tr}\left(\mathbb{E}\left[\mathrm{e}^{-\mathrm{i}W_\beta\cdot p}\Upsilon_\beta^+(W)\right]^*\mathbb{E}\left[\mathrm{e}^{-\mathrm{i}W'_\beta\cdot p}\Upsilon_\beta^+(W')\right]\right)\\
&=\mathbb{E}\left[\mathrm{e}^{\mathrm{i}(W_\beta-W'_\beta)\cdot p}\mathrm{Tr}\left(\Upsilon_\beta^+(W)\Upsilon_\beta^+(W')\right)\right]\\
&\le\mathbb{E}\left[\left(\mathrm{Tr}\left(\left(\Upsilon_\beta^+(W)\right)^2\right)\mathrm{Tr}\left((\Upsilon_\beta^+(W'))^2\right)\right)^{1/2}\right]\\
&\le\mathbb{E}\left[\mathrm{Tr}\left(\left(\Upsilon_\beta^+(W)\right)^2\right)\right]\\
&\le\mathrm{e}^{k\beta}.
\end{aligned}
$$

We also observe that the generalized Weyl's law implies that ρ is in $L^2(\mathbb{R}^{2N},\mathbb{C}^{d\times d})$, namely

$$
\left(\frac{M^{1/2}}{2\pi}\right)^N\int_{\mathbb{R}^{2N}}\mathrm{Tr}\left(\rho^2(z)\right)\mathrm{d}z=\mathrm{Tr}\left(\widehat{\rho}\widehat{\rho}\right)=\mathrm{Tr}\left(\mathrm{e}^{-\beta\widehat{H}}\mathrm{e}^{-\beta\widehat{H}}\right)=\mathrm{Tr}\left(\mathrm{e}^{-2\beta\widehat{H}}\right)<\infty,
$$

which proves (2.22). □

4.3. Proof Lemma 3.2

Proof. To estimate remainder terms we will use the composition operator for Weyl symbols defined by $\widehat{c\#d} = \widehat{c}\widehat{d}$. The composition operator has the representation

$$\begin{aligned} c\#d &= \mathrm{e}^{\frac{\mathrm{i}}{2M^{1/2}}\left(\nabla_{x'}\cdot\nabla_p - \nabla_x\cdot\nabla_{p'}\right)} c(x,p)d(x',p')\big|_{(x,p)=(x',p')} \\ &= \mathrm{e}^{\frac{\mathrm{i}}{2M^{1/2}}\left(\nabla_{x''}\cdot\nabla_{p'} - \nabla_{x'}\cdot\nabla_{p''}\right)} \underbrace{c(x+x',p+p')d(x+x'',p+p'')}_{=:f_{xp}(x',p',x'',p'')}\big|_{(x',p')=(x'',p'')=0} \end{aligned} \tag{4.9}$$

which can be written as an expansion using the Fourier transform $\mathcal{F}$, defined for $f:\mathbb{R}^{4N}\to\mathbb{R}$ by

$$\mathcal{F}\{f\}(\xi_{x'},\xi_{p'},\xi_{x''},\xi_{p''}) := \int_{\mathbb{R}^{4N}} f(x',p',x'',p'')\mathrm{e}^{-\mathrm{i}\left(x'\cdot\xi_{x'}+p'\cdot\xi_{p'}+x''\cdot\xi_{x''}+p''\cdot\xi_{p''}\right)}\,\mathrm{d}x'\,\mathrm{d}p'\,\mathrm{d}x''\,\mathrm{d}p''. \tag{4.10}$$

Its inverse transform implies

$$\begin{aligned} &\mathrm{e}^{-\frac{\mathrm{i}}{2M^{1/2}}\left(\nabla_{x''}\cdot\nabla_{p'} - \nabla_{x'}\cdot\nabla_{p''}\right)} f(x',p',x'',p'')\Big|_{(x',p')=(x'',p'')=0} \\ &\quad = \left(\frac{1}{2\pi}\right)^{4N}\int_{\mathbb{R}^{4N}} \mathcal{F}f(\xi_{x'},\xi_{p'},\xi_{x''},\xi_{p''})\mathrm{e}^{\frac{\mathrm{i}}{2}M^{-1/2}\left(\xi_{x''}\cdot\xi_{p'}-\xi_{x'}\cdot\xi_{p''}\right)}\,\mathrm{d}\xi_{x'}\,\mathrm{d}\xi_{p'}\,\mathrm{d}\xi_{x''}\,\mathrm{d}\xi_{p''} \end{aligned}$$

and Taylor expansion of the exponential function yields

$$\begin{aligned} &\mathrm{e}^{-\frac{\mathrm{i}}{2M^{1/2}}\left(\nabla_{x''}\cdot\nabla_{p'} - \nabla_{x'}\cdot\nabla_{p''}\right)} f_{xp}(x',p',x'',p'')\Big|_{(x',p')=(x'',p'')=0} \\ &\quad = \left(\frac{1}{2\pi}\right)^{4N}\int_{\mathbb{R}^{4N}} \mathcal{F}f_{xp}(\xi_{x'},\xi_{p'},\xi_{x''},\xi_{p''})\mathrm{e}^{\frac{\mathrm{i}}{2}M^{-1/2}\left(\xi_{x''}\cdot\xi_{p'}-\xi_{x'}\cdot\xi_{p''}\right)}\,\mathrm{d}\xi_{x'}\,\mathrm{d}\xi_{p'}\,\mathrm{d}\xi_{x''}\,\mathrm{d}\xi_{p''} \\ &\quad = \left(\frac{1}{2\pi}\right)^{4N}\int_{\mathbb{R}^{2N}} \mathcal{F}f_{xp}(\xi_{x'},\xi_{p'},\xi_{x''},\xi_{p''})\Bigg(\sum_{n=0}^{m}\left(\frac{\mathrm{i}(\xi_{x''}\cdot\xi_{p'}-\xi_{x'}\cdot\xi_{p''})}{2M^{1/2}}\right)^n\frac{1}{n!} \\ &\qquad + \left(\frac{\mathrm{i}(\xi_{x''}\cdot\xi_{p'}-\xi_{x'}\cdot\xi_{p''})}{2M^{1/2}}\right)^{m+1}\times\frac{1}{m!}\int_0^1(1-s)^m\mathrm{e}^{\frac{\mathrm{i}s}{2}M^{-1/2}\left(\xi_{x''}\cdot\xi_{p'}-\xi_{x'}\cdot\xi_{p''}\right)}\,\mathrm{d}s\Bigg)\,\mathrm{d}\xi_{x'}\,\mathrm{d}\xi_{p'}\,\mathrm{d}\xi_{x''}\,\mathrm{d}\xi_{p''} \\ &\quad = \sum_{n=0}^{m}\frac{1}{n!}\left(-\frac{\mathrm{i}(\nabla_{x''}\cdot\nabla_{p'}-\nabla_{x'}\cdot\nabla_{p''})}{2M^{1/2}}\right)^n f_{xp}(x',p',x'',p'')\Big|_{(x,'p')=(x'',p'')=0} \\ &\qquad + \left(\frac{1}{2M^{1/2}}\right)^{m+1}\int_0^1\mathrm{e}^{-\frac{\mathrm{i}s}{2}M^{-1/2}\left(\nabla_{x''}\cdot\nabla_{p'}-\nabla_{x'}\cdot\nabla_{p''}\right)}(-\mathrm{i}(\nabla_{x''}\cdot\nabla_{p'}-\nabla_{x'}\cdot\nabla_{p''}))^{m+1} \\ &\qquad \times f_{xp}(x',p',x'',p'')\frac{(1-s)^m}{m!}\,\mathrm{d}s\Big|_{(x,'p')=(x'',p'')=0}. \end{aligned} \tag{4.11}$$

The pointwise limit of the remainder term can be estimated by dominated convergence

$$\begin{aligned} \lim_{M\to\infty}\int_0^1 &\mathrm{e}^{-\frac{\mathrm{i}s}{2}M^{-1/2}\left(\nabla_{x''}\cdot\nabla_{p'}-\nabla_{x'}\cdot\nabla_{p''}\right)}(-\mathrm{i}(\nabla_{x''}\cdot\nabla_{p'}-\nabla_{x'}\cdot\nabla_{p''}))^{m+1} \\ &\times f_{xp}(x',p',x'',p'')\frac{(1-s)^m}{m!}\,\mathrm{d}s\Big|_{(x,'p')=(x'',p'')=0} \\ &= (-\mathrm{i}(\nabla_{x''}\cdot\nabla_{p'}-\nabla_{x'}\cdot\nabla_{p''}))^{m+1}f_{xp}(x',p',x'',p'')\frac{1}{(m+1)!}\Big|_{(x,'p')=(x'',p'')=0} \end{aligned}$$

provided $\int_{\mathbb{R}^{4N}}|(\xi_{x''}\cdot\xi_{p'}-\xi_{x'}\cdot\xi_{p''})^{m+1}\mathcal{F}f_{xp}(\xi)|\,\mathrm{d}\xi<\infty$. In addition we need convergence in $L^1(\mathbb{R}^{2N})$, as a function of $z=(x,p)$, to apply dominated convergence in the phase-space integrals. We have

$$\mathcal{F}f_{xp}(\xi_{x'},\xi_{p'},\xi_{x''},\xi_{p''}) = \mathcal{F}c(\xi_{x'},\xi_{p'})\mathrm{e}^{\mathrm{i}(x\cdot\xi_{x'}+p\cdot\xi_{p'})}\mathcal{F}d(\xi_{x''},\xi_{p''})\mathrm{e}^{\mathrm{i}(x\cdot\xi_{x''}+p\cdot\xi_{p''})}$$

so that

$$\begin{aligned}
&\int_{\mathbb{R}^{4N}} \mathcal{F}f_{xp}(\xi_{x'},\xi_{p'},\xi_{x''},\xi_{p''})\mathrm{e}^{\frac{\mathrm{i}s}{2}M^{-1/2}\left(\xi_{x''}\cdot\xi_{p'}-\xi_{x'}\cdot\xi_{p''}\right)}\,\mathrm{d}\xi_{x'}\,\mathrm{d}\xi_{p'}\,\mathrm{d}\xi_{x''}\,\mathrm{d}\xi_{p''}\\
&\quad=\int_{\mathbb{R}^{4N}}\Big(1-\Delta_{\xi_{x'}}-\Delta_{\xi_{p'}}\Big)^k\Big(1-\Delta_{\xi_{x''}}-\Delta_{\xi_{p''}}\Big)^k(\mathcal{F}c(\xi_{x'},\xi_{p'})\mathcal{F}d(\xi_{x''},\xi_{p''})\\
&\quad\times\mathrm{e}^{\frac{\mathrm{i}s}{2}M^{-1/2}\left(\xi_{x''}\cdot\xi_{p'}-\xi_{x'}\cdot\xi_{p''}\right)}\Big)\times\frac{\mathrm{e}^{\mathrm{i}\left(x\cdot\xi_{x''}+p\cdot\xi_{p''}\right)}}{(1+|x''|^2+|p''|^2)^k}\frac{\mathrm{e}^{\mathrm{i}\left(x\cdot\xi_{x'}+p\cdot\xi_{p'}\right)}}{(1+|x'|^2+|p'|^2)^k}\,\mathrm{d}\xi_{x'}\,\mathrm{d}\xi_{p'}\,\mathrm{d}\xi_{x''}\,\mathrm{d}\xi_{p''}.
\end{aligned}$$

Therefore we obtain remainder terms that are uniformly bounded in $L^1(\mathbb{R}^{2N})$ provided the Fourier transform $(\mathrm{i}\xi)^\alpha\mathcal{F}c(\xi)$ of $\partial_z^\alpha c(z)$ satisfies

$$\int_{\mathbb{R}^{2N}}\Big|(1-\Delta_\xi)^{N+1}(\xi^\alpha\mathcal{F}c(\xi))\Big|\,\mathrm{d}\xi<\infty \tag{4.12}$$

and similarly for d

$$\int_{\mathbb{R}^{2N}}\Big|(1-\Delta_\xi)^{N+1}(\xi^\alpha\mathcal{F}d(\xi))\Big|\,\mathrm{d}\xi<\infty.$$

We will apply the composition expansion to functions in the Schwartz class so that (4.12) holds.

We conclude that Schwartz functions c and d satisfy

$$\begin{aligned}
\lim_{M\to\infty}\left(M\left(\frac{c\#d+d\#c}{2}-cd\right)\right)&=\lim_{M\to\infty}\left(-\frac14\int_0^1\cos\Big(\frac{s}{2M^{1/2}}\nabla_z\cdot\nabla'_{z'}\Big)(\nabla_z\cdot\nabla'_{z'})^2c(z)d(z')\big|_{z=z'}(1-s)\,\mathrm{d}s\right)\\
&=-\frac18(\nabla_z\cdot\nabla'_{z'})^2c(z)d(z')\big|_{z=z'},
\end{aligned}\tag{4.13}$$

and

$$\lim_{M\to\infty}(c\#d)=\lim_{M\to\infty}\left(cd-\frac{\mathrm{i}}{2M^{1/2}}\int_0^1\mathrm{e}^{\frac{\mathrm{i}s}{2M^{1/2}}\nabla_z\cdot\nabla'_{z'}}(\nabla_z\cdot\nabla'_{z'})c(z)d(z')\big|_{z=z'}\,\mathrm{d}s\right)=cd, \tag{4.14}$$

as limits in $L^1(\mathbb{R}^{2N})$ and in $L^\infty(\mathbb{R}^{2N})$. We also have

$$\widehat{Da_s}=\mathrm{i}M^{1/2}\Big[\widehat{H},\widehat{a_s}\Big]-\widehat{\{h,a_s\}}=\widehat{\{H-h,a_s\}}+\hat{r}_s^a$$

where

$$r_s^a=\frac{1}{8M}\int_0^1\cos\Big(\frac{\bar{s}}{2M^{1/2}}\nabla_z\cdot\nabla'_{z'}\Big)(\nabla_z\cdot\nabla'_{z'})^3H(z)a_s(z')\big|_{z=z'}(1-\bar{s})^2\,\mathrm{d}\bar{s} \tag{4.15}$$

so that

$$\lim_{M\to\infty}Mr_s^a=\frac{1}{24}\Big(\nabla_{z_0}\cdot\nabla'_{z'_0}\Big)^3H(z_0)a_0(z_s(z'_0))\big|_{z_0=z'_0}$$

and the Poisson bracket takes the form

$$\begin{aligned}
\{H-h,a_s\}&=\nabla'_{z'_0}\cdot\nabla_{z_0}(H-h)(z'_0)a_0(z_s(z_0))\big|_{z_0=z'_0}\\
&=(\nabla_{p'_0}\cdot\nabla_{x_0}-\nabla_{x'_0}\cdot\nabla_{p_0})(H-h)(x'_0,p'_0)a_0(z_s(x_0,p_0))\big|_{(x_0,p_0)=(x'_0,p'_0)}.
\end{aligned}$$

Based on this remainder estimate there holds

$$\begin{aligned}
\mathrm{Tr}\left(\Big(\widehat{Da_s}\Big)^2\widehat{\rho}\right)=\left(\frac{\sqrt{M}}{2\pi}\right)^N\int_{\mathbb{R}^{2N}}\mathrm{Tr}\Big(\Big(\mathrm{i}M^{1/2}(H\#a_s-a_s\#H)-\{h,a_s\}\Big)\\
\#\Big(\mathrm{i}M^{1/2}(H\#a_s-a_s\#H)-\{h,a_s\}\Big)\,\rho\Big)\,\mathrm{d}z
\end{aligned}$$

and in the limit we obtain by (4.14), (4.15) and Lemma 2.3

$$\begin{aligned}\lim_{M\to\infty}\int_{\mathbb{R}^{2N}}\operatorname{Tr}\Big(\Big(\mathrm{i}M^{1/2}(H\#a_s-a_s\#H)-\{h,a_s\}\Big)\\ \#\Big(\mathrm{i}M^{1/2}(H\#a_s-a_s\#H)-\{h,a_s\}\Big)\ \rho\Big)\,\mathrm{d}z\\ =\int_{\mathbb{R}^{2N}}\operatorname{Tr}\Big(\nabla_{z_0}a\big(z_s(z_0)\cdot\nabla'_{z_0}(H-h)\big)^2\mathrm{e}^{-\beta H(z_0)}\Big)\,\mathrm{d}z_0,\end{aligned}$$

using splitting of the phase space integral as in (3.12), which together with (4.13)–(4.15) and Lemma 4.1 below proves the lemma. □

Lemma 4.1. *Assume that the bounds in Theorem 2.1 hold, then a_t and b_t are in the Schwartz class and there is a constant C', depending in C, such that*

$$\sum_{|\alpha|\le 3}\|\partial_z^\alpha a_t(z)\|_{L^\infty(\mathbb{R}^{2N})}+\sum_{|\alpha|\le 3}\|\partial_z^\alpha b_t(z)\|_{L^\infty(\mathbb{R}^{2N})}\le C'. \tag{4.16}$$

Proof. To estimate $\sum_{|\alpha|\le 3}\|\partial_{p_0}^\alpha a_0(z_t(z_0))\|_{L^\infty(\mathbb{R}^{2N})}$ we use the first order flow $\nabla_{z_0}z_t(z_0)=:z'(t)$, second order flow $z''_{,km}(t)=\partial_{z_k(0)z_m(0)}z(t)$ and third order flow $z'''(t)$, which are solutions to the system

$$\begin{aligned}\dot z_i(t)&=\big(\nabla'_{z_t}h(z_t)\big)_i=:f_i(z_t),\\ z'_{i,k}(t)&=\mathrm{I}_{ik}+\int_0^t\sum_{k'}f'_{i,k'}(z_s)z'_{k',k}(s)\,\mathrm{d}s,\quad f'_{i,k'}(z):=\partial_{z_{k'}}f_i(z),\\ z''_{i,km}(t)&=\int_0^t\Big(\sum_{k'}f'_{i,k'}(z_s)z''_{k',km}(s)+\sum_{k'm'}f''_{i,k'm'}(z_s)z'_{k',k}(s)z'_{m',m}(s)\Big)\,\mathrm{d}s,\\ &\qquad f''_{i,k'm'}(z):=\partial_{z_{k'}z_{m'}}f_i(z),\\ z'''_{i,kmn}(t)&=\int_0^t\Big(\sum_{k'}f'_{i,k'}(z_s)z'''_{k',kmn}(s)+\sum_{k'm'}f''_{i,k'm'}(z_s)z'_{k',k}(s)z''_{m',mn}(s)\\ &\quad+\sum_{k'm'}f''_{i,k'm'}(z_s)z''_{k',kn}(s)z'_{m',m}(s)+\sum_{k'n'}f''_{i,k'n'}(z_s)z''_{k',km}(s)z'_{n',n}(s)\\ &\quad+\sum_{k'm'n'}f'''_{i,k'm'n'}(z_s)z'_{k',k}(s)z'_{m',m}(s)z'_{n',n}(s)\Big)\,\mathrm{d}s.\end{aligned}$$

By summation and maximization over indices we obtain the integral inequalities

$$\begin{aligned}\max_{ik}\big|z'_{i,k}(t)\big|&\le 1+\int_0^t\sum_{k'}\big|f'_{i,k'}(z_s)\big|\max_{ik}\big|z'_{i,k}(s)\big|\,\mathrm{d}s,\\ \max_{ik}\sum_m|z''_{i,km}(t)|&\le\int_0^t\sum_{k'}\big|f'_{i,k'}(z_s)\big|\max_{ik}\sum_m\big|z''_{i,km}(s)\big|\,\mathrm{d}s+\int_0^t\sum_{k'm'}\big|f''_{i,k'm'}(z_s)\big|\Big(\max_{ik}\big|z'_{i,k}(s)\big|\Big)^2\,\mathrm{d}s,\\ \max_{ik}\sum_{mn}|z'''_{i,kmn}(t)|&\le\int_0^t\sum_{k'}\big|f'_{i,k'}(z_s)\big|\max_{ik}\sum_{mn}\big|z'''_{i,kmn}(s)\big|\,\mathrm{d}s\\ &\quad+\int_0^t\sum_{k'm'}\big|f''_{i,k'm'}(z_s)\big|\max_{ik}\big|z'_{i,k}(s)\big|\max_{ik}\sum_m\big|z''_{i,km}(s)\big|\,\mathrm{d}s\end{aligned}$$

$$+\int_0^t \sum_{k'm'n'} \left|f'''_{i,k'm'n'}(z_s)\right| \left(\max_{ik} \left|z'_{i,k}(s)\right|\right)^3 \mathrm{d}s. \tag{4.17}$$

The functions $\max_{ij} \sum_{|\alpha|\leq 2} \partial^\alpha_{z_0} \partial_{z_j} z_i(t, z_0)$ can therefore be estimated as in [23] by Gronwall's inequality, which states: if there is a positive constant K and continuous positive functions $\gamma, u : [0, \infty) \to [0, \infty)$ such that

$$u(t) \leq K + \int_0^t \gamma(s) u(s)\, \mathrm{d}s, \qquad \text{for } t > 0,$$

then

$$u(t) \leq K \mathrm{e}^{\int_0^t \gamma(s)\, \mathrm{d}s}, \qquad \text{for } t > 0.$$

Gronwall's inequality applied to (4.17) implies

$$\max_{ij} \sum_{|\alpha|\leq 2} \left\|\partial^\alpha_{z_0} \partial_{z_j} z_i(t, z_0)\right\|_{L^\infty(\mathbb{R}^{2N})} = \mathcal{O}(1) \tag{4.18}$$

provided that

$$\max_{i} \sum_{|\alpha|\leq 3} \|\partial^\alpha_x \partial_{x_i} h\|_{L^\infty(\mathbb{R}^N)} = \mathcal{O}(1). \tag{4.19}$$

The flows z', z'', z''' determine the derivatives of the scalar symbol $a_0(z_t(z_0)) = a_t(z_0)$

$$\begin{aligned}
\partial_{z_k} a_t &= \sum_{k'} a'_{0,k'}(z_t) z'_{k',k}(t), \qquad a'_{0,k'}(z) := \partial_{z_{k'}} a_0(z), \\
\partial_{z_k z_m} a_t &= \sum_{k'} a'_{0,k'}(z_t) z''_{k',km}(t) + \sum_{k'm'} a''_{0,k'm'}(z_t) z'_{k',k}(t) z'_{m',m}(t), \\
\partial_{z_k z_m z_n} a_t &= \sum_{k'} a'_{0,k'}(z_t) z'''_{k',kmn}(t) + \sum_{k'm'} a''_{0,k'm'}(z_t) z'_{k',k}(t) z''_{m',mn}(t) \\
&\quad + \sum_{k'm'} a''_{0,k'm'}(z_t) z''_{k',kn}(t) z'_{m',m}(t) + \sum_{k'n'} a''_{0,k'n'}(z_t) z''_{k',km}(t) z'_{n',n}(t) \\
&\quad + \sum_{k'm'n'} a'''_{0,k'm'n'}(z_t) z'_{k',k}(t) z'_{m',m}(t) z'_{n',n}(t),
\end{aligned} \tag{4.20}$$

which together with (4.18) proves (4.16).

Similarly to verify that a_t is a Schwartz function, we first extend both (4.17) (for $\partial^\alpha_{z_0} z_t(z_0)$) and the representation in (4.20) to order $|\alpha|$ to obtain the bounds

$$|\partial^\alpha_z a_t(z)| < \infty, \tag{4.21}$$

for all indices α. Then define the compact set $\mathbb{L}^c_m = \{z \in \mathbb{R}^{2N} : h(z) \leq m\}$. The property $h(z) \to \infty$ as $|z| \to \infty$, which is verified below (3.13), implies that L^c_m includes the support of a_0 for m sufficiently large and the invariance $h(z_t(z_0)) = h(z_0)$, for all $z_0 \in \mathbb{R}^{2N}$, establishes by (4.21)

$$\sup_{z\in\mathbb{R}^{2N}} |z^\gamma \partial^\alpha_z a_t(z)| = \sup_{z\in L^c_m} |z^\gamma \partial^\alpha_z a_0(z_t(z))| < \infty,$$

for all indices γ and α. We conclude that a_t is a Schwartz function. □

The constant in the right hand side of (4.18) grows typically exponentially with respect to t, *i.e.*,

$$\max_{ij} \sum_{|\alpha|\leq 2} \left\|\partial^\alpha_{z_0} \partial_{z_j} z_i(t, z_0)\right\|_{L^\infty(\mathbb{R}^{2N})} \leq \mathrm{e}^{c' t},$$

where c' is the positive constant in the right hand side of (4.19). We note that the assumptions on h and V are compatible with the assumption to have $\int_{\mathbb{R}^{2N}} \mathrm{Tr}\, \mathrm{e}^{-\beta H(z)}\, \mathrm{d}z$ bounded.

5. Numerical experiments

In this section we define a model problem that allows us to systematically study approximation of canonical quantum correlation observables. The model problem is constructed so that we can accurately approximate the quantum dynamics, thereby avoiding the computational challenges to accurately approximate realistic quantum systems with many particles and excited electron states, *cf.* [24]. Section 5.1 includes the approximations of equilibrium density function of position observable $\hat{x}$, applying the mean-field molecular dynamics and the electron ground state molecular dynamics, respectively. In Section 5.2, we compare time-dependent correlation observables obtained from molecular dynamics evolving on the ground state, on the mean-field energy surface, and on a weighted average of all eigenstates (denoted the excited state dynamics below). In particular, we study whether the mean-field approximation can be more accurate than using only the ground state.

In order to demonstrate the proposed mean-field molecular dynamics approximation, we devise the model problem as described by equations (1.12) to (1.14) in Section 1.2, where the difference between two eigenvalues $\lambda_1(x) - \lambda_0(x) = 2c\sqrt{x^2+\delta^2}$ can be tuned by the two parameters c and δ. For δ small this model relates to the avoided crossing phenomenon in quantum chemistry where the two potential surfaces get almost intersected at a certain point, see [1]. The assumptions in Theorem 2.1 are satisfied for positive δ but not for $\delta = 0$ and therefore the approximation error is expected to vary with different δ.

5.1. Equilibrium observables

At the inverse temperature β, the quantum canonical ensemble average of a time-independent observable $\hat{A}$ is obtained from the normalized trace

$$\frac{\mathrm{Tr}\left(\mathrm{e}^{-\beta\hat{H}}\hat{A}\right)}{\mathrm{Tr}\left(\mathrm{e}^{-\beta\hat{H}}\right)} = \frac{\sum_n \mathrm{e}^{-\beta E_n}\left\langle \Phi_n,\, \hat{A}\Phi_n\right\rangle}{\sum_n \mathrm{e}^{-\beta E_n}}, \tag{5.1}$$

where $(E_n, \Phi_n)_{n=1}^{\infty}$ are eigenvalues and the corresponding normalized eigenstates of the Hamiltonian operator $\widehat{H}$. Consequently, for an observable depending only on the position x with symbol $A(x)$, we have

$$\frac{\mathrm{Tr}\left(\mathrm{e}^{-\beta\hat{H}}\hat{A}\right)}{\mathrm{Tr}\left(\mathrm{e}^{-\beta\hat{H}}\right)} = \int_{\mathbb{R}^N} A(x)\,\mu_{\mathrm{qm}}(x)\,\mathrm{d}x, \quad \text{where} \quad \mu_{\mathrm{qm}}(x) = \frac{\sum_n |\Phi_n(x)|^2 \mathrm{e}^{-\beta E_n}}{\sum_n \mathrm{e}^{-\beta E_n}}. \tag{5.2}$$

We apply a fourth-order finite difference scheme for the Laplacian operator in the Hamiltonian (1.12) to approximate the equilibrium density $\mu_{\mathrm{qm}}(x)$ in (5.2). The numerical implementation is explained with more details in Appendix A.1.

As an approximation to the quantum canonical ensemble average (5.1), we consider the normalized trace $\mathrm{Tr}\,(\widehat{\mathrm{e}^{-\beta H}}\,\widehat{A})\,/\,\mathrm{Tr}\,(\widehat{\mathrm{e}^{-\beta H}})$ and apply the Lemma 2.2 and equation (1.16) to write the mean-field observable as

$$\begin{aligned}\mathfrak{T}_{\mathrm{md}}(0) = \mathfrak{T}_{\mathrm{es}}(0) &= \frac{\mathrm{Tr}\left(\widehat{\mathrm{e}^{-\beta H}}\,\widehat{A}\right)}{\mathrm{Tr}\left(\widehat{\mathrm{e}^{-\beta H}}\right)} = \frac{\int_{\mathbb{R}^{2N}} \mathrm{Tr}\big(\mathrm{e}^{-\beta H(x,p)} a(x,p)\mathrm{I}\big)\,\mathrm{d}x\,\mathrm{d}p}{\int_{\mathbb{R}^{2N}} \mathrm{Tr}\big(\mathrm{e}^{-\beta H(x',p')}\big)\,\mathrm{d}x'\,\mathrm{d}p'} \\ &= \frac{\int_{\mathbb{R}^{2N}} a(x,p)\big(\mathrm{e}^{-\beta\lambda_0(x)} + \mathrm{e}^{-\beta\lambda_1(x)}\big)\,\mathrm{e}^{-\frac{\beta|p|^2}{2}}\,\mathrm{d}x\,\mathrm{d}p}{\int_{\mathbb{R}^{2N}} \big(\mathrm{e}^{-\beta\lambda_0(x')} + \mathrm{e}^{-\beta\lambda_1(x')}\big)\,\mathrm{e}^{-\frac{\beta|p'|^2}{2}}\,\mathrm{d}x'\,\mathrm{d}p'},\end{aligned}$$

where $H(x,p)$ and $A(x,p) = a(x,p)\mathrm{I}$ with $a : \mathbb{R}^{2N} \to \mathbb{C}$ are the Weyl symbols corresponding to the operators $\hat{H}$ and $\hat{A}$, respectively.

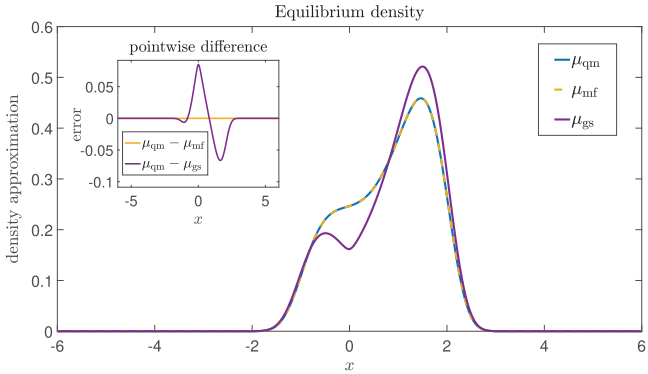

FIGURE 2. The density functions computed with the quantum mechanics formula (5.2), the mean-field approximation formula (5.3), and using only the ground state in the classical formula (5.5), with mass ratio $M = 1000$. The mean-field density (the dashed yellow line) is quite close to the quantum mechanics density curve (the solid blue line), implying a better accuracy than the ground state density (the solid violet line).

Specifically for an observable depending only on the position x, we obtain

$$\frac{\mathrm{Tr}\left(\widehat{\mathrm{e}^{-\beta H}}\,\widehat{A}\right)}{\mathrm{Tr}\left(\widehat{\mathrm{e}^{-\beta H}}\right)} = \int_{\mathbb{R}^N} A(x)\,\mu_{\rm mf}(x)\,\mathrm{d}x, \quad \text{where} \quad \mu_{\rm mf}(x) = \frac{\mathrm{e}^{-\beta\lambda_0(x)} + \mathrm{e}^{-\beta\lambda_1(x)}}{\int_{\mathbb{R}^N}\left(\mathrm{e}^{-\beta\lambda_0(x')} + \mathrm{e}^{-\beta\lambda_1(x')}\right)\mathrm{d}x'}. \tag{5.3}$$

The classical mean-field density $\mu_{\rm mf}$ in (5.3) can also be rewritten as a weighted average

$$\mu_{\rm mf}(x) = \sum_{j=0}^{1} q_j \,\frac{\mathrm{e}^{-\beta\lambda_j(x)}}{\int_{\mathbb{R}}\mathrm{e}^{-\beta\lambda_j(x')}\,\mathrm{d}x'}, \quad \text{where} \quad q_j = \frac{\int_{\mathbb{R}^N}\mathrm{e}^{-\beta\lambda_j(x)}\,\mathrm{d}x}{\sum_{k=0}^{1}\int_{\mathbb{R}^N}\mathrm{e}^{-\beta\lambda_k(x)}\,\mathrm{d}x}, \ j = 0, 1. \tag{5.4}$$

The weights q_0 and q_1 can be interpreted as the probability for the system to be in the corresponding electron eigenstate λ_0 and λ_1, respectively obtained by integration with the corresponding Gibbs density.

We first plot the equilibrium quantum mechanics density $\mu_{\rm qm}$ using the formula (5.2), and compare it with the classical mean-field density $\mu_{\rm mf}$ in (5.3). They are also compared with the density based only on the ground state $\mu_{\rm gs}$, with the formula

$$\mu_{\rm gs}(x) = \frac{\mathrm{e}^{-\beta\lambda_0(x)}}{\int_{\mathbb{R}^N}\mathrm{e}^{-\beta\lambda_0(x)}\,\mathrm{d}x}, \tag{5.5}$$

which is obtained from the classical density formula (5.4) by taking the probability for the excited state as $q_1 = 0$, and the probability for the ground state as $q_0 = 1$.

In Figure 2 the first reference density curve with quantum mechanics formula (5.2) is plotted in blue colour with a solid line. The density curve $\mu_{\rm mf}(x)$, obtained from the classical mean-field formula (5.3), is plotted as the yellow dashed line and agrees well with the quantum mechanics density $\mu_{\rm qm}(x)$. Besides, the mean-field density $\mu_{\rm mf}(x)$ incurs much smaller error than the ground-state density $\mu_{\rm gs}(x)$ (the violet solid curve) in approximating the $\mu_{\rm qm}(x)$ density. For Figure 2, we use the parameters $M = 1000$, $c = 1$, and $\beta = 1$ such that with the eigenvalue gap $\delta = 0.1$, the system has a probability $q_1 = 0.16$ to be in the excited state.

In Figure 3 we depict a point-wise difference between the classical mean-field density $\mu_{\rm mf}(x)$ and the quantum mechanics density $\mu_{\rm qm}(x)$, for different values of the mass ratio M. The inverse temperature is still taken as $\beta = 1$ for the eigenvalue gap $\delta = 0.1$ and $c = 1$, so that the probability for the excited state is kept as $q_1 = 0.16$.

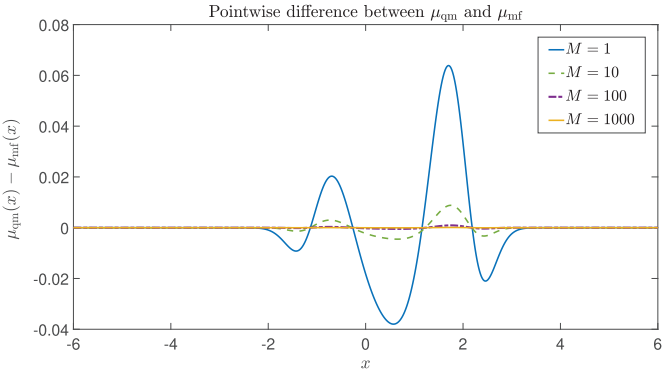

FIGURE 3. The point-wise difference between the quantum mechanics density $\mu_{\rm qm}$ and the mean-field density $\mu_{\rm mf}$ with inverse temperature $\beta = 1$. The dashed violet curve with $M = 100$ has so small an error that it is almost indiscernible from the solid yellow curve with $M = 1000$.

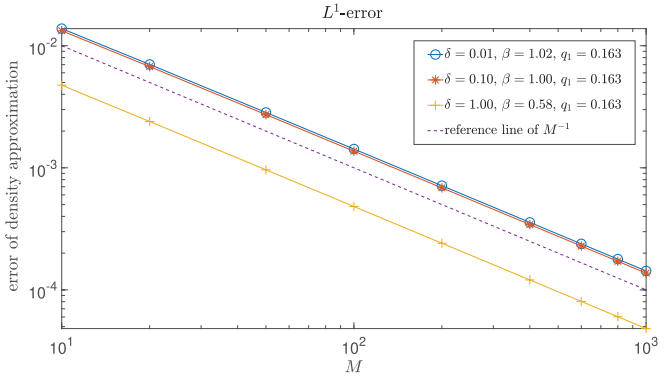

FIGURE 4. Dependence of the L^1-error between the quantum density $\mu_{\rm qm}$ and the classical mean-field density approximation $\mu_{\rm mf}$, shown in log-log scale.

It is observed from Figure 3 that as M increases the error in the classical mean-field density approximation decreases.

In order to study the dependence of the approximation error $\|\mu_{\rm qm} - \mu_{\rm mf}\|_{L^1}$ on the mass ratio M, we vary M for three different inverse temperatures, with the corresponding eigenvalue gaps δ such that the probability to be in the excited state remains to be $q_1 = 0.16$. As seen from Figure 4, the $\mathcal{O}(M^{-1})$ dependence of the error in the equilibrium density using the classical mean-field approximation is in accordance with the theoretical result of Theorem 2.1.

Besides the M-dependence of the classical approximation, we also experiment with a relatively large inverse temperature $\beta = 10$ for mass ratio $M = 100$, with parameters $c = 1$, $\delta = 0.1$. The quantum density $\mu_{\rm qm}$ together with its classical mean-field and ground state approximations $\mu_{\rm mf}$ and $\mu_{\rm gs}$ are plotted in the Figure 5. The large value of β implies a rather low temperature, which leads to a tiny probability for the electron excited state as $q_1 = 7 \times 10^{-7}$. Consequently the density functions concentrate near the minimum of the ground state eigenvalue, and there is almost no difference between the mean-field and the ground state density curves.

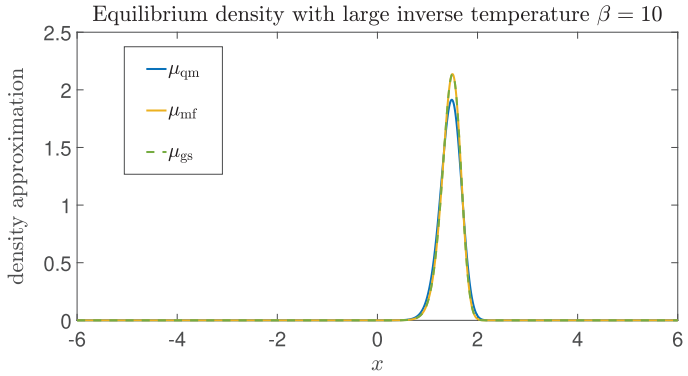

FIGURE 5. Equilibrium density $\mu_{\rm qm}$ with the classical mean-field and ground state approximations $\mu_{\rm mf}$ and $\mu_{\rm gs}$, with inverse temperature $\beta = 10$, mass ratio $M = 100$. The probability of electron excited state $q_1 = 7 \times 10^{-7}$ is tiny.

5.2. Time-correlated observables

5.2.1. The model problem

We apply the mean-field molecular dynamics to approximate the auto-correlation function between the momentum observables $\widehat{p}_0$ (at time 0) and $\widehat{p}_\tau$ (at time τ). In the Heisenberg representation the time evolution of the momentum observable is given by

$$\widehat{p}_\tau := \mathrm{e}^{\mathrm{i}\tau\sqrt{M}\widehat{H}}\widehat{p}_0\mathrm{e}^{-\mathrm{i}\tau\sqrt{M}\widehat{H}}.$$

We study the two-eigenvalue model with the potential matrix $V(x)$ as defined by (1.13) in Section 1.2. For computing the quantum correlation function, we approximate the initial position observable $\widehat{x}_0$ and the initial momentum observable $\widehat{p}_0$ by the matrices

$$\widehat{x}_0 \simeq \begin{bmatrix} x_0 & & & & & & \mathbf{0} \\ & x_0 & & & & & \\ & & x_1 & & & & \\ & & & x_1 & & & \\ & & & & \ddots & & \\ & & & & & x_K & \\ \mathbf{0} & & & & & & x_K \end{bmatrix} =: X, \quad \widehat{p}_0 \simeq \mathrm{i}\sqrt{M}(H_d X - X H_d) =: P,$$

respectively, where we discretize a sufficiently large computational domain $\Omega = [x_0, x_K]$ with uniform grid points $x_k = x_0 + k\Delta x$, for $k = 0, 1, \cdots, K$ and $\Delta x = \frac{|x_K - x_0|}{K}$. In the definition of the matrix P, the real symmetric matrix H_d is of size $2(K+1) \times 2(K+1)$, corresponding to a fourth order finite difference approximation of the Hamiltonian operator $\widehat{H}$. More details about this approximation are provided in Section A.1, and the definition of matrix H_d is given in (A.2). The matrix H_d generates the approximations

$$\mathrm{e}^{\mathrm{i}\tau\sqrt{M}\widehat{H}} \simeq \mathrm{e}^{\mathrm{i}\tau\sqrt{M}H_d}, \quad \mathrm{e}^{-\beta\widehat{H}} \simeq \mathrm{e}^{-\beta H_d}.$$

We apply the `eig` function of `Matlab` to obtain the eigenpairs (e_n, ϕ_n) of the H_d matrix, and rearrange them to obtain the eigendecomposition

$$Q := \begin{bmatrix} \phi_1 & \phi_2 & \phi_3 & \cdots & \phi_{2(K+1)} \end{bmatrix}, \text{ and } D := \begin{bmatrix} e_1 & & & \mathbf{0} \\ & e_2 & & \\ & & \ddots & \\ \mathbf{0} & & & e_{2(K+1)} \end{bmatrix},$$

such that H_d can be diagonalized with the orthogonal matrix Q as $H_d = Q\,D\,Q^*$, and hence

$$\mathrm{e}^{\mathrm{i}\tau\sqrt{M}H_d} = Q\,\mathrm{e}^{\mathrm{i}\tau\sqrt{M}D}\,Q^*, \quad \text{and} \quad \mathrm{e}^{-\beta H_d} = Q\,\mathrm{e}^{-\beta D}\,Q^*.$$

Thus the right-hand side of (1.3) with $\widehat{A}_\tau = \widehat{p}_\tau$ and $\widehat{B}_0 = \widehat{p}_0$ can be approximated by

$$\begin{aligned}\mathfrak{T}_{\mathrm{qm}}(\tau) &:= \frac{\mathrm{Tr}\left((\widehat{p}_\tau\,\widehat{p}_0 + \widehat{p}_0\,\widehat{p}_\tau)\,\mathrm{e}^{-\beta\widehat{H}}\right)}{2\,\mathrm{Tr}\left(\mathrm{e}^{-\beta\widehat{H}}\right)} = \frac{\mathrm{Tr}\left(\widehat{p}_\tau\left(\widehat{p}_0\,\mathrm{e}^{-\beta\widehat{H}} + \mathrm{e}^{-\beta\widehat{H}}\,\widehat{p}_0\right)\right)}{2\,\mathrm{Tr}\left(\mathrm{e}^{-\beta\widehat{H}}\right)} \\ &\simeq \frac{\mathrm{Tr}\left(Q\,\mathrm{e}^{\mathrm{i}\tau\sqrt{M}D}\,Q^*\,P\,Q\,\mathrm{e}^{-\mathrm{i}\tau\sqrt{M}D}\,Q^*\left(P\,Q\,\mathrm{e}^{-\beta D}\,Q^* + Q\,\mathrm{e}^{-\beta D}\,Q^*\,P\right)\right)}{2\,\mathrm{Tr}\left(Q\,\mathrm{e}^{-\beta D}\,Q^*\right)},\end{aligned} \tag{5.6}$$

where in the second equality we use the cyclic property of the trace.

By applying the mean-field molecular dynamics formula (1.4) with momentum observables $\widehat{p}_0$ and $\widehat{p}_\tau$ in the model problem, we have the approximation for the time-correlation function as

$$\mathfrak{T}_{\mathrm{mf}}(\tau) = \frac{\int_{\mathbb{R}^{2N}} p_\tau p_0\,\mathrm{Tr}\left(\mathrm{e}^{-\beta H(z_0)}\right)\mathrm{d}z_0}{\int_{\mathbb{R}^{2N}}\mathrm{Tr}\left(\mathrm{e}^{-\beta H(z_0)}\right)\mathrm{d}z_0}, \tag{5.7}$$

where $z_t := (x_t, p_t)$ solves the Hamiltonian system

$$\begin{aligned}\dot{x}_t &= \nabla_p\,h(x_t,p_t), \\ \dot{p}_t &= -\nabla_x\,h(x_t,p_t),\end{aligned} \tag{5.8}$$

with an initial state $z_0 = (x_0, p_0) \in \mathbb{R}^2$.

The Hamiltonian system (5.8) is solved numerically with the second-order velocity Verlet scheme, see [25]. More details about this numerical implementation is in Appendix A.2.

We also apply the classical molecular dynamics formula for correlation functions introduced in Section 2.3.2 of [2], which considers the contribution from the ground state and the excited states. For our specific example the *excited state dynamics* approximation of momentum correlation observable is given by

$$\mathfrak{T}_{\mathrm{es}}(\tau) := \sum_{j=0}^{1}\int_{\mathbb{R}^2} q_j\,p_\tau^j(z_0)\,p_0^j(z_0)\,\frac{\mathrm{e}^{-\beta\left(\frac{|p_0|^2}{2}+\lambda_j(x_0)\right)}}{\int_{\mathbb{R}^2}\mathrm{e}^{-\beta\left(\frac{|p|^2}{2}+\lambda_j(x)\right)}\,\mathrm{d}z}\,\mathrm{d}z_0,, \tag{5.9}$$

with the weights q_0 and q_1 as defined in (5.4), where $z_\tau^j = (x_\tau^j, p_\tau^j)$, $j = 0, 1$ solves the Hamiltonian dynamics

$$\begin{aligned}\dot{x}_\tau^j &= p_\tau^j, \\ \dot{p}_\tau^j &= -\nabla\lambda_j(x_\tau^j),\end{aligned}$$

with the initial condition $z_0^j = (x_0, p_0) = z_0$ and $\lambda_0(x)$, $\lambda_1(x)$ as defined in (1.14).

In addition to these three expressions for time-correlation, $\mathfrak{T}_{\mathrm{qm}}$ (the quantum mechanics correlation), $\mathfrak{T}_{\mathrm{mf}}$ (the mean-field approximation), and $\mathfrak{T}_{\mathrm{es}}$ (the classical excited state approximation), we also compute the approximation based only on the ground state contribution, $\mathfrak{T}_{\mathrm{gs}}$, obtained by setting the probability q_1 for the excited state equal to be zero, *i.e.*,

$$\mathfrak{T}_{\mathrm{gs}}(\tau) = \int_{\mathbb{R}^2} p_\tau(z_0)\,p_0(z_0)\,\frac{\mathrm{e}^{-\beta\left(\frac{|p_0|^2}{2}+\lambda_0(x_0)\right)}}{\int_{\mathbb{R}^2}\mathrm{e}^{-\beta\left(\frac{|p|^2}{2}+\lambda_0(x)\right)}\,\mathrm{d}z}\,\mathrm{d}z_0, \tag{5.10}$$

where $z_\tau = (x_\tau, p_\tau)$ solves the Hamiltonian dynamics with the potential $\lambda_0(x)$

$$\begin{aligned} \dot{x}_\tau &= p_\tau, \\ \dot{p}_\tau &= -\nabla\lambda_0(x_\tau), \end{aligned}$$

with initial state $z_0 = (x_0, p_0)$.

As discussed in (1.16), the approximations with mean-field dynamics or excited state dynamics at an initial time $\tau = 0$ are always identical, *i.e.*, $\mathfrak{T}_{\rm mf}(0) = \mathfrak{T}_{\rm es}(0)$. For position-related observables, the classical ground state dynamics approximation $\mathfrak{T}_{\rm gs}(0)$ will be, in general, different from $\mathfrak{T}_{\rm mf}(0)$ and $\mathfrak{T}_{\rm es}(0)$, which is consistent with our preceding observations on equilibrium density function in Section 5.1, and is confirmed in the upcoming Figure 13.

The numerical approximations of $\mathfrak{T}_{\rm mf}(\tau)$, $\mathfrak{T}_{\rm es}(\tau)$, and $\mathfrak{T}_{\rm gs}(\tau)$ are computed with the Verlet method in combination with Simpson's formula. We use $\mathcal{S}_{\rm mf}(\tau)$, $\mathcal{S}_{\rm es}(\tau)$, $\mathcal{S}_{\rm gs}(\tau)$, and $\mathcal{S}_{\rm qm}(\tau)$, to denote the numerical approximations of $\mathfrak{T}_{\rm mf}(\tau)$, $\mathfrak{T}_{\rm es}(\tau)$, $\mathfrak{T}_{\rm gs}(\tau)$, and $\mathfrak{T}_{\rm qm}(\tau)$, respectively.

In practise ground state molecular dynamics in the canonical ensemble is relatively well developed for realistic molecular systems and successful mean-field approximations appear in centroid and ring-polymer molecular dynamics [26]. Direct computations of excited state dynamics for realistic systems seem less attractive, due to the challenge to efficiently compute excited electron states, *cf.* [24]. Here we compare these three alternatives for a simple model problem in the hope of giving some information also on realistic systems.

5.2.2. Numerical results

Following the discussion on the variances ϵ_1^2 and ϵ_2^2 with equations (1.8), (1.10) and (1.11), we survey five different cases with varying parameter settings of c, δ, and inverse temperature β, and make a comparison between the performances of different molecular dynamics approximations in each case. A summary of the parameters in each case is given in the Table 1.

Case A: ***Low temperature with large eigenvalue gap***, $\beta = 3.3$, $c = 1$, $\delta = 1$, $\epsilon_1^2 = 9.95 \times 10^{-4}$, $\epsilon_2^2 = 1.25 \times 10^{-4}$, the probability for the excited state $q_1 = 0.0002$ is almost negligible.

Figure 6a presents the eigenvalues $\lambda_0(x)$, $\lambda_1(x)$ and the mean-field potential function $\lambda_*(x)$ as defined in (1.9) for Case A. With the parameters $c = 1$ and $\delta = 1$, the system has a large eigenvalue gap. Particularly in this low temperature setting, the mean-field potential $\lambda_*(x)$ is almost identical to the ground-state eigenvalue $\lambda_0(x)$. Since the probability for the excited state is very small ($q_1 = 0.0002$), the three molecular dynamics approximations $\mathfrak{T}_{\rm mf}(\tau)$, $\mathfrak{T}_{\rm es}(\tau)$, and $\mathfrak{T}_{\rm gs}(\tau)$ are similar.

In Figure 7a, the quantum mechanics correlation function curve $\mathcal{S}_{\rm qm}(\tau)$ with mass ratio $M = 1000$ is plotted as a function of correlation time τ, together with the three molecular dynamics approximations $\mathcal{S}_{\rm mf}(\tau)$, $\mathcal{S}_{\rm es}(\tau)$, and $\mathcal{S}_{\rm gs}(\tau)$. The three molecular dynamics correlation function curves are almost on top of each other, as shown in Figure 7b with similarly small errors. This case gives an example where all the three molecular dynamics work analogously, since $q_1 \ll 1$, and we note that the error terms ϵ_1^2, ϵ_2^2 together with $1/M$ are all very small.

Case B: ***High temperature with small difference between eigenvalues***, $\beta = 1$, $c = 0.1$, $\delta = 1$, $\epsilon_1^2 = 1.9 \times 10^{-2}$, $\epsilon_2^2 = 3.5 \times 10^{-3}$, the probability for the excited state $q_1 = 0.43$.

In Figure 6b we observe that with the parameter setting of case B, the mean-field potential $\lambda_*(x)$ lies in between the ground state eigenvalue $\lambda_0(x)$ and the excited state eigenvalue $\lambda_1(x)$, indicating that by incorporating the effect of the excited state, the mean-field approximation $\mathfrak{T}_{\rm mf}(\tau)$ can make a difference from simply using the ground state molecular dynamics.

The improved accuracy of the mean-field molecular dynamics is verified by the Figure 8b, in which we observe a smaller error of mean-field molecular dynamics approximation $\|\mathcal{S}_{\rm qm} - \mathcal{S}_{\rm mf}\|_{L^\infty([0,\tau])}$ (the red curve) compared with the molecular dynamics using only the ground state $\|\mathcal{S}_{\rm qm} - \mathcal{S}_{\rm gs}\|_{L^\infty([0,\tau])}$ (the violet curve). The excited state molecular dynamics $\mathcal{S}_{\rm es}(\tau)$ has the smallest error, manifesting an effective combination of the information from both the ground and the excited eigenstates.

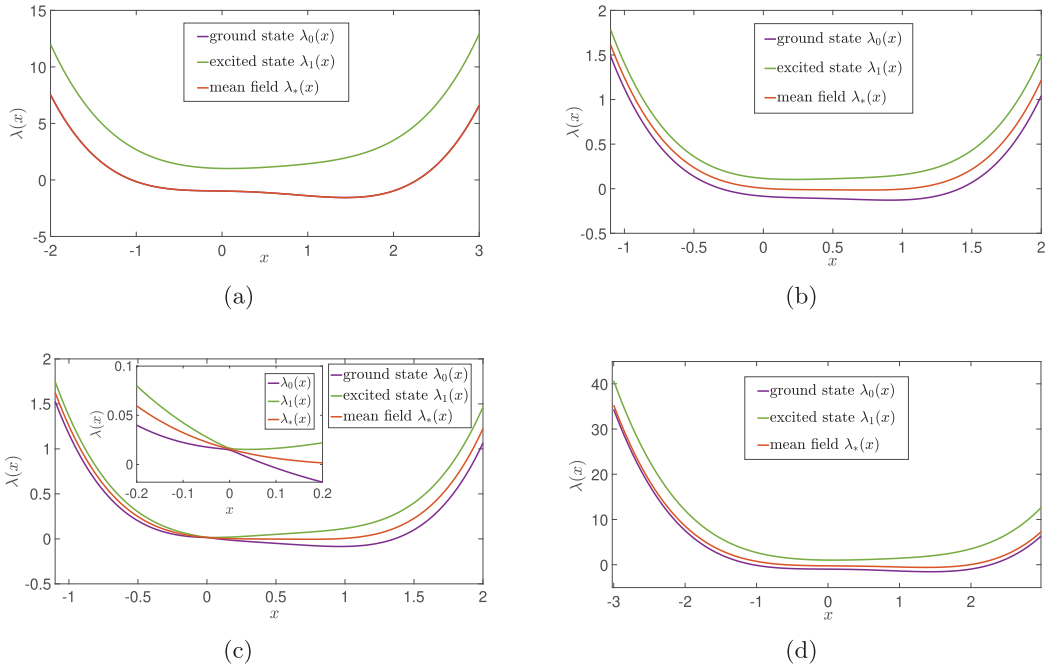

FIGURE 6. Eigenvalues of the matrix-valued potential $V(x)$ for test cases A to D. In the panel (a), the mean-field potential $\lambda_*(x)$ (the red curve) is quite close to the ground state $\lambda_0(x)$ (the violet curve). (a) Case A: low temperature, large difference between eigenvalues, large gap. (b) Case B: high temperature, small difference between eigenvalues, small gap. (c) Case C: high temperature, small difference between eigenvalues, smallest gap. (d) Case D: high temperature, large difference between eigenvalues, medium gap.

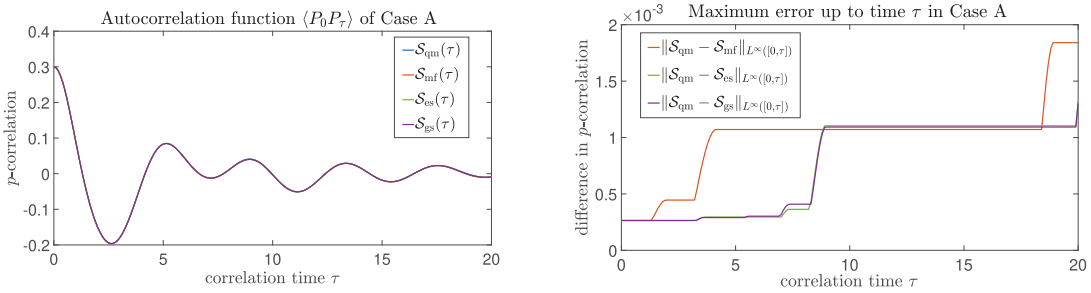

FIGURE 7. Case A: (a) Auto-correlation function $\langle P_0 P_\tau \rangle$ computed by quantum-mechanics formula, $\mathcal{S}_{\rm qm}$, with $M = 1000$, and by three molecular dynamics formulae. (b) The corresponding maximum errors up to time τ, $\|\mathcal{S}_{\rm qm} - \mathcal{S}_{\rm md}\|_{L^\infty([0,\tau])}$.

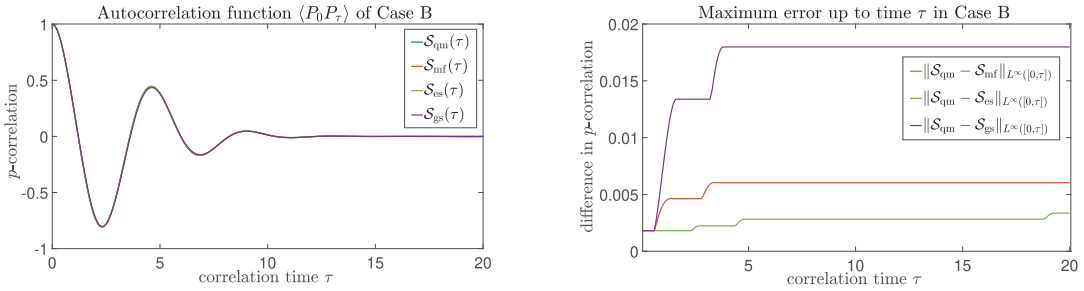

(a) (b)

FIGURE 8. Case B: (a) Auto-correlation function $\langle P_0 P_\tau \rangle$ computed by quantum-mechanics formula, $\mathcal{S}_{\rm qm}$, with $M = 100$, and by three molecular dynamics formulae. (b) The corresponding maximum errors up to time τ $\|\mathcal{S}_{\rm qm} - \mathcal{S}_{\rm md}\|_{L^\infty([0,\tau])}$.

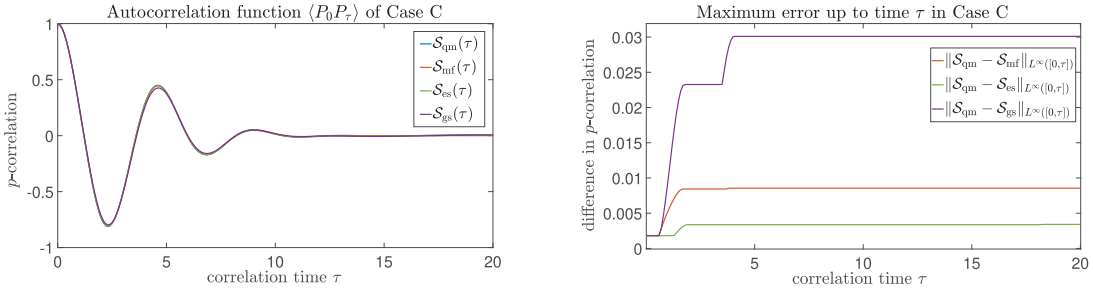

(a) (b)

FIGURE 9. Case C: (a) Auto-correlation function $\langle P_0 P_\tau \rangle$ computed by quantum-mechanics formula, $\mathcal{S}_{\rm qm}$, with $M = 100$, and by three molecular dynamics formulae. (b) The corresponding maximum errors up to time τ $\|\mathcal{S}_{\rm qm} - \mathcal{S}_{\rm md}\|_{L^\infty([0,\tau])}$.

Case C: ***High temperature, small difference between eigenvalues with avoided crossing***, $\beta = 1$, $c = 0.1$, $\delta = 0.01$, $\epsilon_1^2 = 9.1 \times 10^{-3}$, $\epsilon_2^2 = 9.9 \times 10^{-3}$, the probability for the excited state $q_1 = 0.46$.

The Case C has a similar parameter setting as the preceding Case B, with the only difference of a smaller parameter $\delta = 0.01$. The small parameter δ leads to a small eigenvalue gap at $x = 0$, *i.e.*, the two eigenvalues $\lambda_0(x)$ and $\lambda_1(x)$ almost intersect at this point, as can be seen in the Figure 6c. Compared with Case B, the small eigenvalue gap also makes the probability for the excited state q_1 increase from 0.43 to 0.46 in Case C, with the same inverse temperature $\beta = 1$.

The approximate p-auto-correlation function curves with their corresponding maximum errors up to time τ are plotted in the Figures 9a and 9b, respectively. These two figures are quite similar to their corresponding plots in Case B, where the excited state approximation $\mathcal{S}_{\rm es}$ has the smallest error, and the mean-field approximation $\mathcal{S}_{\rm mf}$ achieves an improved accuracy compared to the ground state approximation $\mathcal{S}_{\rm gs}$.

The similar approximation error of the three molecular dynamics in Case B and Case C can be understood as a result of the relatively small difference between the two eigenvalues λ_0 and λ_1. For both cases the small parameter $c = 0.1$ leads to small ϵ_1 and ϵ_2 values, as summarized in Table 1.

Case D: ***High temperature, large difference between eigenvalues with large gap***, $\beta = 0.28$, $c = 1$, $\delta = 1$, $\epsilon_1^2 = 2.01$, $\epsilon_2^2 = 0.42$, the probability for the excited state $q_1 = 0.30$.

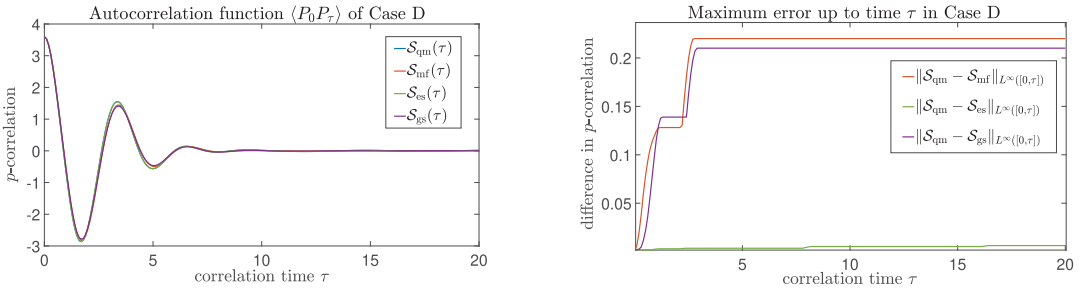

FIGURE 10. Case D: (a) Auto-correlation function $\langle P_0 P_\tau \rangle$ computed by quantum-mechanics formula, $\mathcal{S}_{\rm qm}$, with $M = 100$, and by three molecular dynamics formulae. (b) The corresponding maximum errors up to time τ $\|\mathcal{S}_{\rm qm} - \mathcal{S}_{\rm md}\|_{L^\infty([0,\tau])}$.

For this case, we observe from Figure 6d that although the mean-field potential $\lambda_*(x)$ is still in between the ground state $\lambda_0(x)$ and the excited state $\lambda_1(x)$, the distance between $\lambda_*(x)$ and $\lambda_1(x)$ is much larger than that in the previous Case B. Also $\lambda_*(x)$ is much closer to the ground state $\lambda_0(x)$ than to the excited state $\lambda_1(x)$. The parameter $\beta = 0.28$ implies a relatively high temperature, with a considerable contribution from the excited state. Hence we cannot expect the mean-field molecular dynamics to be much better than ground state molecular dynamics. This is also verified by Figure 10b which shows that the error of mean-field molecular dynamics is of the same order as that of ground state molecular dynamics, while the excited state molecular dynamics remains accurate.

The mean-field and ground state molecular dynamics correlations include two approximations: replacing the matrix-valued potential $V(x)$ by a scalar potential $\lambda_*(x)$ or $\lambda_0(x)$ respectively, and replacing quantum dynamics with classical dynamics,

$$\begin{aligned} \mathcal{S}_{\rm qm}(\tau) - \mathcal{S}_{\rm mf}(\tau) &= (\mathcal{S}_{\rm qm}(\tau) - \mathcal{S}_{{\rm qm},\lambda_*}(\tau)) + (\mathcal{S}_{{\rm qm},\lambda_*}(\tau) - \mathcal{S}_{\rm mf}(\tau)) \\ \mathcal{S}_{\rm qm}(\tau) - \mathcal{S}_{\rm gs}(\tau) &= (\mathcal{S}_{\rm qm}(\tau) - \mathcal{S}_{{\rm qm},\lambda_0}(\tau)) + (\mathcal{S}_{{\rm qm},\lambda_0}(\tau) - \mathcal{S}_{\rm gs}(\tau)) \end{aligned} \tag{5.11}$$

where $\mathcal{S}_{{\rm qm},\lambda_*}$ and $\mathcal{S}_{{\rm qm},\lambda_0}$ denote the approximation of auto-correlation function computed with quantum dynamics but using scalar-valued potentials $\lambda_*(x)$ and $\lambda_0(x)$, respectively. In the right hand side of (5.11), the first terms $(\mathcal{S}_{\rm qm}(\tau) - \mathcal{S}_{{\rm qm},\lambda_*}(\tau))$ and $(\mathcal{S}_{\rm qm}(\tau) - \mathcal{S}_{{\rm qm},\lambda_0}(\tau))$ correspond to the potential approximations in quantum dynamics, while the second terms $(\mathcal{S}_{{\rm qm},\lambda_*}(\tau) - \mathcal{S}_{\rm mf}(\tau))$ and $(\mathcal{S}_{{\rm qm},\lambda_0}(\tau) - \mathcal{S}_{\rm gs}(\tau))$ are related to classical approximations of quantum dynamics using scalar potentials.

To investigate these two error contributions we compute the correlation function $\mathcal{S}_{{\rm qm},\lambda_*}(\tau)$ and $\mathcal{S}_{{\rm qm},\lambda_0}(\tau)$ for Case D, using the scalar-valued potential $\lambda_*(x)$ or $\lambda_0(x)$ to replace the potential matrix $V(x)$ in the quantum dynamics. The corresponding auto-correlation curves and their maximum error up to time τ are shown in Figures 11a and 11b.

From Figure 11b, we clearly see that the errors $\|\mathcal{S}_{\rm qm} - \mathcal{S}_{{\rm qm},\lambda_*}\|_{L^\infty([0,\tau])}$ and $\|\mathcal{S}_{\rm qm} - \mathcal{S}_{{\rm qm},\lambda_0}\|_{L^\infty([0,\tau])}$ caused by substituting the potential matrix $V(x)$ with the scalar-valued potentials $\lambda_*(x)$ or $\lambda_0(x)$ is of the same order as the total errors $\|\mathcal{S}_{\rm qm} - \mathcal{S}_{\rm mf}\|_{L^\infty([0,\tau])}$ and $\|\mathcal{S}_{\rm qm} - \mathcal{S}_{\rm gs}\|_{L^\infty([0,\tau])}$ in Figure 10b. Hence we conclude that the main source of error in this case is the simplification by replacing the potential matrix $V(x)$ with a scalar-valued potential, and not the approximation of scalar potential quantum mechanics correlation by classical molecular dynamics.

We also vary the mass ratio M between the heavy particle and the light particle, in order to study the corresponding behaviour of the approximation errors $\|\mathcal{S}_{\rm qm}(\tau) - \mathcal{S}_{{\rm qm},\lambda_*}(\tau)\|_{L^\infty([0,\tau])}$ and $\|\mathcal{S}_{\rm qm}(\tau) - \mathcal{S}_{{\rm qm},\lambda_0}(\tau)\|_{L^\infty([0,\tau])}$ up to time $\tau = 20$ for the mean-field molecular dynamics and ground state molecular dynamics in Case D. As

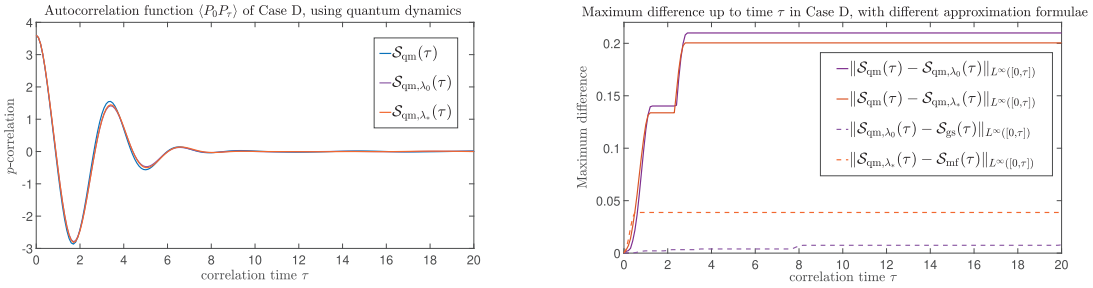

(a) (b)

FIGURE 11. (a) Auto-correlation function $\langle P_0 P_\tau \rangle$ curves $\mathcal{S}_{\rm qm}$, $\mathcal{S}_{{\rm qm},\lambda_0}$, and $\mathcal{S}_{{\rm qm},\lambda_*}$ computed by using matrix valued potential $V(x)$, and using scalar-valued potential $\lambda_0(x)$ or $\lambda_*(x)$ in the quantum mechanics formula (5.6) in Case D. (b) Maximum error up to time τ in the p-auto-correlation curves computed with quantum mechanics formula using scalar-valued potential $\lambda_*(x)$ or $\lambda_0(x)$, by comparing them with the correlation computed from quantum mechanics formula using matrix-valued potential $V(x)$, and with their corresponding molecular dynamics approximations.

TABLE 2. Case D: Dependence of the error on the mass ratio M at time $\tau = 20$.

M	$\|\mathcal{S}_{\rm qm} - \mathcal{S}_{{\rm qm},\lambda_*}\|$	$\|\mathcal{S}_{{\rm qm},\lambda_*} - \mathcal{S}_{\rm mf}\|$	$\|\mathcal{S}_{\rm qm} - \mathcal{S}_{{\rm qm},\lambda_0}\|$	$\|\mathcal{S}_{{\rm qm},\lambda_0} - \mathcal{S}_{\rm gs}\|$	$\|\mathcal{S}_{\rm qm} - \mathcal{S}_{\rm es}\|$
100	0.2004	0.0387	0.2099	0.0081	0.0062
50	0.1985	0.0384	0.2080	0.0201	0.0220
20	0.1944	0.0375	0.2033	0.0377	0.0330

can be seen from the second and fourth column of Table 2, the main error caused by substitution of the potential matrix V with the scalar valued potential λ_* or λ_0 varies slightly as the M value changes.

Case E: ***High temperature, large difference between eigenvalues with avoided crossing***, with $\beta = 1$, $c = 1$, $\delta = 0.1$, $\epsilon_1^2 = 0.29$, $\epsilon_2^2 = 0.50$, the probability for the excited state $q_1 = 0.16$.

This case has the same parameters as in Section 5.1. In Figure 1 we observe a pattern of the two eigenvalues $\lambda_0(x)$ and $\lambda_1(x)$ related to avoided crossing of potential surfaces. Our numerical results suggest that for this case all three molecular dynamics are only accurate for short time, as can be seen in Figure 12a. Compared to Case C and Case D, where the excited state dynamics is accurate, the diminished eigenvalue regularity at the avoided crossing may explain the loss of accuracy in Case E.

Apart from the momentum auto-correlation function, we also computed in Case E the correlation function between position observables $\widehat{x}_0$ and $\widehat{x}_\tau$, as plotted in Figure 13. We observe that for short time range (*e.g.*, $0 \leq \tau \leq 0.1$), the error of the ground state molecular dynamics is larger than the error of the mean-field molecular dynamics, which is consistent with the result for equilibrium observables in Section 5.1, in which the ground state molecular dynamics has larger error in approximating the density function $\mu_{\rm qm}(x)$ than the mean-field formula. Therefore the mean-field molecular dynamics can improve short-time approximation of position auto-correlation function compared to the ground state molecular dynamics.

We also changed the mass ratio M in this case for the momentum auto-correlation function, from $M = 100$ to $M = 50$ and to smaller value $M = 20$. When M becomes smaller, we can expect the error of molecular dynamics approximation becomes larger, since the error includes the $\mathcal{O}(M^{-1})$ term. For Case E, since we are only interested in the short time approximation, the time-dependent error term is not much larger than the $\mathcal{O}(M^{-1})$ term. Hence the effect of varying the mass ratio M will be considerable. The dependence of the L^∞-

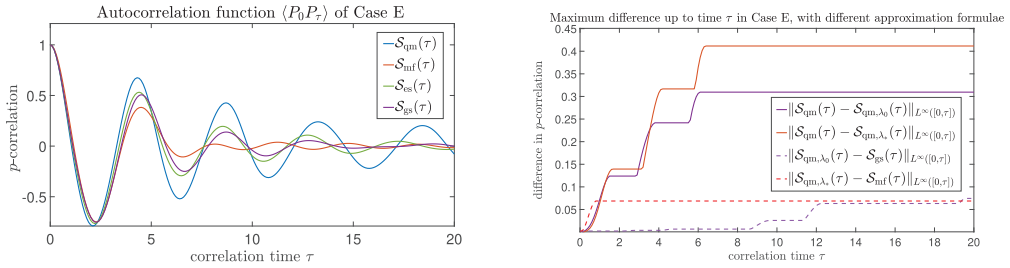

(a) (b)

FIGURE 12. (a) Auto-correlation function $\langle P_0 P_\tau \rangle$ curves $\mathcal{S}_{\rm qm}$, $\mathcal{S}_{{\rm qm},\lambda_0}$, and $\mathcal{S}_{{\rm qm},\lambda_*}$ computed by using matrix valued potential $V(x)$ and using scalar-valued potential $\lambda_0(x)$ or $\lambda_*(x)$ in the quantum mechanics formula (5.6) in Case E. (b) Maximum error up to time τ in the p-auto-correlation curves computed with quantum mechanics formula using scalar-valued potential $\lambda_*(x)$ or $\lambda_0(x)$, by comparing them with the correlation computed from quantum mechanics formula using matrix-valued potential $V(x)$, and with their corresponding molecular dynamics approximations.

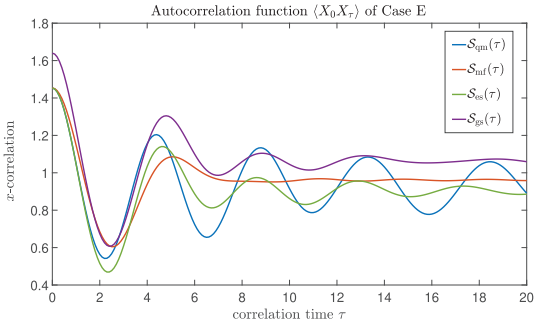

FIGURE 13. Case E: Auto-correlation function $\langle X_0 X_\tau \rangle$ computed by quantum-mechanics formula with $M = 100$ and by three molecular dynamics formulae.

TABLE 3. Case E: Dependence of the error on the mass ratio M at different correlation times τ.

τ	M	$\|\mathcal{S}_{\rm qm} - \mathcal{S}_{\rm mf}\|_{L^\infty([0,\tau])}$	$\|\mathcal{S}_{\rm qm} - \mathcal{S}_{\rm es}\|_{L^\infty([0,\tau])}$	$\|\mathcal{S}_{\rm qm} - \mathcal{S}_{\rm gs}\|_{L^\infty([0,\tau])}$
1	20	0.1375	0.0816	0.0564
1	50	0.1324	0.0766	0.0513
1	100	0.1270	0.0712	0.0460
2	20	0.1657	0.1515	0.1043
2	50	0.1533	0.1356	0.0884
2	100	0.1425	0.1226	0.0759

error in momentum auto-correlation approximation on the mass ratio M is summarized in Table 3, from which we observe an improved accuracy in all the three molecular dynamics approximations with an increased M value.

5.3. Conclusion from numerical comparisons

From the study with equilibrium observables in Section 5.1, we see that by considering the contributions of excited states the classical mean-field approximation of quantum mechanics density at equilibrium achieves a substantial improvement from the approximation which uses only the information from the ground state. The error of the mean-field approximation will decrease as the mass ratio M increases, following the $\mathcal{O}(M^{-1})$ relation.

For the time-dependent observables, specifically by studying the momentum auto-correlation function, we know from Case A that for a low temperature setting with a large eigenvalue gap, where the probability for an excited state is small, all three molecular dynamics with the mean-field approximation, excited state approximation, or ground state approximation work similarly well.

From Case B and Case D, we observe that the error of the mean-field approximation decreases as the difference between two eigenvalues diminishes (*i.e.*, parameter c becomes small). Furthermore, for Case B with a small difference between two eigenvalues, the mean-field approximation improves the accuracy of molecular dynamics compared to using the ground state only.

With a small eigenvalue difference, even including the avoided crossing in Case C the result is similar to Case B, that is the mean-field approximation is still more accurate than the ground state approximation.

From Case D we know that when the system temperature is high and the difference between two eigenvalues is not small, the excited state approximation outperforms both the mean-field and the ground state molecular dynamics.

From Case E we see that when the difference between the eigenvalues are sufficiently large and when the potential matrix includes avoided crossings, all three molecular dynamics approximations are accurate for a short time range only.

The small error terms ϵ_1^2 and ϵ_2^2, in Table 1, for the Cases A, B and C is consistent with the actual error being small for the mean-field approximation, while in Cases D and E where the mean-field approximation error is large these error terms are in fact large. Therefore the experiments indicate that the error estimate could be useful to estimate the mean-field approximation error also for realistic problems when the quantum observable is not computable.

Figures 11b and 12b together with Table 2 show that in Case D and Case E, where mean-field and ground state approximations are not accurate, the error of the mean-field and ground state molecular dynamics are dominated by the matrix valued potential replaced by a scalar potential on the quantum level, since the classical approximation error of the quantum dynamics for the corresponding scalar potential is clearly smaller.

Appendix A. Numerical implementations

A.1. Finite difference approximation of the equilibrium density

To approximate the quantum mechanics density formula (5.2), we use a fourth-order finite difference approximation of the Laplacian in the Hamiltonian operator $\widehat{H}$ (5.1), with the formula

$$f''(x) = \frac{-f(x-2h) + 16f(x-h) - 30f(x) + 16f(x+h) - f(x+2h)}{12h^2} + \mathcal{O}(h^4).$$

This discretization is performed on the computational domain $\Omega = [-6, 6]$ with a uniform mesh $x_k = -6 + k\Delta x$, for $k = 0, 1, \cdots, K$, with $\Delta x = \frac{12}{K}$. The choice of this computational domain is obtained by checking that the quantum mechanics density $\mu_{\rm qm}(x)$ approximately vanishes on the boundary of this domain, so that the homogeneous Dirichlet boundary condition can be assumed. By applying this discretization, we approximate the eigenvalue problem

$$\widehat{H}\Phi_n = E_n\Phi_n,$$

with the following algebraic eigenvalue problem

$$H_d\phi_n = e_n\phi_n, \tag{A.1}$$

where the $2(K+1)\times 2(K+1)$ matrix H_d is given by

$$H_d := \frac{1}{2M\cdot 12(\Delta x)^2} \times \begin{bmatrix} h_{11,0}+30 & h_{12,0} & -16 & 0 & 1 & & & & & & \\ h_{21,0} & h_{22,0}+30 & 0 & -16 & 0 & 1 & & & & & \\ -16 & 0 & h_{11,1}+30 & h_{12,1} & -16 & 0 & 1 & & & & \\ 0 & -16 & h_{21,1} & h_{22,1}+30 & 0 & -16 & 0 & 1 & & & \\ 1 & 0 & -16 & 0 & h_{11,2}+30 & h_{12,2} & -16 & 0 & 1 & & \\ & 1 & 0 & -16 & h_{21,2} & h_{22,2}+30 & 0 & -16 & 0 & 1 & \\ & & \ddots & \ddots & \ddots & \ddots & \ddots & \ddots & \ddots & \ddots & \ddots \\ & & & 1 & 0 & -16 & 0 & h_{11,K-1}+30 & h_{12,K-1} & -16 & 0 \\ & & & & 1 & 0 & -16 & h_{21,K-1} & h_{22,K-1}+30 & 0 & -16 \\ & & & & & 1 & 0 & -16 & 0 & h_{11,K}+30 & h_{12,K} \\ & & & & & & 1 & 0 & -16 & h_{21,K} & h_{22,K}+30 \end{bmatrix} \tag{A.2}$$

and the eigenfunctions Φ_n are approximated with the $2(K+1)$-length vector ϕ_n, as

$$\phi_n = [\phi_{n,0,1}, \phi_{n,0,2}, \phi_{n,1,1}, \phi_{n,1,2}, \cdots, \phi_{n,K,1}, \phi_{n,K,2}]^T.$$

Here, the entry terms $h_{ij,k}$ of the H_d matrix are given by

$$h_{ij,k} = 2M\big(12\Delta x^2\big)V_{ij}(x_k), \quad \text{for } i,j=1,2, \text{ and } k=0,1,\cdots,K.$$

In practice, based on the finite difference scheme (A.1), we approximate the quantum mechanics density $\mu_{\rm qm}$ in (5.2) by

$$\frac{\sum_n \Big(|\phi_{n,k,1}|^2+|\phi_{n,k,2}|^2\Big)\mathrm{e}^{-\beta e_n}}{\sum_k\sum_n \Big(|\phi_{n,k,1}|^2+|\phi_{n,k,2}|^2\Big)\mathrm{e}^{-\beta e_n}\Delta x}, \quad \text{for} \quad k=0,1,\cdots,K, \tag{A.3}$$

and the eigenvalues e_n and eigenvectors ϕ_n here are obtained by using the `Matlab` function `eig`.

A.2. Numerical solution of the mean-field Hamiltonian system

In the mean-field trace formula (5.7) for time correlation function $\mathcal{S}_{\rm mf}(\tau)$, we need to solve the Hamiltonian system

$$\begin{aligned} \dot{x}_t &= \nabla_p h(x_t,p_t),\\ \dot{p}_t &= -\nabla_x h(x_t,p_t), \end{aligned}$$

to obtain the state variable x_τ at time $t=\tau$. Specifically, given the initial state (x_0,p_0) at time $t_0=0$, we apply the velocity Verlet method, where for each discrete time point $t_n := t_0+n\Delta t$, the dynamics of state variables (x,p) in (1.5) is approximated by

$$\begin{aligned} p_{n+\frac{1}{2}} &= p_n + \frac{\Delta t}{2}\cdot(-\nabla_x h(x_n,p_n)),\\ x_{n+1} &= x_n + \Delta t\cdot p_{n+\frac{1}{2}},\\ p_{n+1} &= p_{n+\frac{1}{2}} + \frac{\Delta t}{2}\cdot\Big(-\nabla_x h\Big(x_{n+1},p_{n+\frac{1}{2}}\Big)\Big). \end{aligned}$$

The integrals in molecular dynamics formulas (5.7), (5.9), and (5.10) are computed with a fourth-order composite Simpson's method, with a discretized mesh $x_l = x_0+l\Delta x$, $p_l = p_0+l\Delta p$, for $l=0,1,\cdots L$ on the phase space (x,p) and the computational domain $\Omega=[x_0,x_L]\times[p_0,p_L]$ is taken to be sufficiently large, with $\Delta x = (x_L-x_0)/L$, $\Delta p=(p_L-p_0)/L$.

Acknowledgements. This research was supported by Swedish Research Council grant 2019-03725 and KAUST grant OSR-2019-CRG8-4033.3. The work of P.P. was supported in part by the U.S. Army Research Office Grant W911NF-19-1-0243.

References

[1] E. Teller, The crossing of potential surfaces. *J. Phys. Chem.* **41** (1937) 109–116.
[2] A. Kammonen, P. Plecháč, M. Sandberg and A. Szepessy, Canonical quantum observables for molecular systems approximated by ab initio molecular dynamics. *Ann. Henri Poincare* **19** (2018) 2727–2781.
[3] R.F. Feynman, Statistical Mechanics: A Set of Lectures. Westview Press, Boulder, CO (1998).
[4] G. Morandi, F. Napoli and E. Ercolessi, Statistical Mechanics: An Intermediate Course. World Scientific Publishing, Singapore (2001).
[5] G.W. Ford and M. Kac, On the quantum Langevin equation. *J. Statist. Phys.* **46** (1987) 803–810.
[6] H. Hoel and A. Szepessy, Classical Langevin dynamics derived from quantum mechanics. *Discrete Continuous Dyn. Syst. B* **25** (2020) 4001–4038.
[7] J.-P. Hansen and I.R. McDonald, Theory of Simple Liquids. Academic Press, London and New York (1985).
[8] H.-M. Stiepan and S. Teufel, Semiclassical approximations for Hamiltonians with operator-valued symbols. *Comm. Math. Phys.* **320** (2013) 821–849.
[9] E. Wigner, On the quantum correction for thermodynamic equilibrium. *Phys. Rev.* **40** (1932) 749–759.
[10] P.-L. Lions and T. Paul, Sur les mesures de Wigner. *Revista Matemática Iberoamericana* **9** (1993) 553–618.
[11] A. Figalli, M. Ligabò and T. Paul, Semiclassical limit for mixed states with singular and rough potentials. *Indiana Univ. Math. J.* **61** (2012) 193–222.
[12] M. Zworski, Semiclassical Analysis. American Mathematical Society, Providence, RI (2012).
[13] A. Martinez, An Introduction to Semiclassical and Microlocal Analysis. Springer Verlag, New York (2002).
[14] A. Bouzounia and D. Robert, Uniform semiclassical estimates for the propagation of quantum observables. *Duke Math. J.* **111** (2002) 223–252.
[15] G. François and T. Paul, Semiclassical evolution with low regularity. *J. Math. Pures App.* **151** (2021) 257–311.
[16] S. Habershon, D.E. Manolopoulos, T.E. Markland and T.F. Miller 3rd., Ring-polymer molecular dynamics: quantum effects in chemical dynamics from classical trajectories in an extended phase space. *Ann. Rev. Phys. Chem.* **64** (2013) 387–413.
[17] A. Pérez, M.E. Tuckerman and M.H. Müser, A comparative study of the centroid and ring-polymer molecular dynamics methods for approximating quantum time correlation functions from path integrals. *J. Chem. Phys.* **130** (2009) 184105.
[18] T. Dornheim, S. Groth, A.V. Filinov and M. Bonitz, Path integral Monte Carlo simulation of degenerate electrons: permutation-cycle properties. *J. Chem. Phys.* **151** (2019) 014108.
[19] L.C. Evans, Partial Differential Equation. American Mathematical Society, Providence, RI (1998).
[20] L. Amour, L. Jager and J. Nourrigat, The Weyl symbol of Schrödinger semigroups. *Ann. Henri Poincare* **16** (2015) 1479–1488.
[21] G. Papanicolaou and R. Hersh, Non-commuting random evolutions, and an operator-valued Feynman–Kac formula. *Comm. Pure Appl. Math.* **XXV** (1972) 337–367.
[22] I. Karatzas and S.E. Shreve, Brownian Motion and Stochastic Calculus. Springer Verlag, New York (1998).
[23] T.H. Gronwall, Note on the derivatives with respect to a parameter of the solutions of a system of differential equations. *Ann. Math.* **20** (1919) 292–296.
[24] E. Cancès, C. Le Bris and P.-L. Lions, Molecular simulation and related topics: some open mathematical problems. *Nonlinearity* **21** (2008) T165–T176.
[25] B. Leimkuhler and C. Matthews, Molecular Dynamics: With Deterministic and Stochastic Numerical Methods. Springer, Berlin (2015).
[26] D. Marx and J. Hutter, Ab Initio Molecular Dynamics: Basic Theory and Advanced Methods. Cambridge University Press, Cambridge (2009).